Quantifying the effects of the division of labor in metabolic pathways

Emily Harvey[*,a,b,1], Jeffrey Heys[b], Tomáš Gedeon[a]

[a] *Mathematical Sciences, Montana State University, Bozeman, Montana 59715*
[b] *Chemical and Biological Engineering, Montana State University, Bozeman, Montana 59715*

Abstract

Division of labor is commonly observed in nature. There are several theories that suggest diversification in a microbial community may enhance stability and robustness, decrease concentration of inhibitory intermediates, and increase efficiency. Theoretical studies to date have focused on proving when the stable co-existence of multiple strains occurs, but have not investigated the productivity or biomass production of these systems when compared to a single 'super microbe' which has the same metabolic capacity. In this work we prove that if there is no change in the growth kinetics or yield of the metabolic pathways when the metabolism is specialised into two separate microbes, the biomass (and productivity) of a binary consortia system is always less than that of the equivalent monoculture. Using a specific example of *Escherichia coli* growing on a glucose substrate, we find that increasing the growth rates or substrate affinities of the pathways is not sufficient to explain the experimentally observed productivity increase in a community. An increase in pathway efficiency (yield) in specialised organisms provides the best explanation of the observed increase in productivity.

Key words: microbial ecology, mathematical modelling, syntrophic consortia, cross-feeding, chemostat

1. Introduction

From the earliest observations of microbial organisms, it has been apparent that microbial consortia are ubiquitous in nature. In fact, naturally occurring ecosystems are almost exclusively organized as consortia. Recent metagenomic studies from the soil [19], to the ocean [66], to the human gut [22], have found

[*]Corresponding author. Telephone: +64 9 4140800 extn.41554
Email addresses: e.p.harvey@massey.ac.nz (Emily Harvey), jeffrey.heys@coe.montana.edu (Jeffrey Heys), gedeon@math.montana.edu (Tomáš Gedeon)
[1]Present address: Institute of Natural and Mathematical Sciences, Massey University Albany, Auckland, New Zealand.

that microbial communities are incredibly diverse, often consisting of thousands of interacting species. Subsets of these communities form *consortia* that act together to enhance their capabilities and survival [14].

Early theoretical ecology studies led to the development of the *competitive exclusion principle* (CEP), which states that the maximum number of species that can coexist in a system is equal to the total number of limiting (essential) resources [26, 37, 49]. However, in nature we see many examples of multiple microbial species stably coexisting. Frequent explanations for coexistence in a natural population can be categorized into three main types: the development of multiple niches due to spatial heterogeneity or self organized segregation, the system not being in equilibrium due to environmental fluctuations or external forcing, and the presence of inter- and intra-species interactions. Despite the limited direct applicability of CEP to natural systems, the clear mathematical formulation of CEP allows for significant insight by identifying which conditions of the CEP have been violated to lead to the observed coexistence of species. For example, by applying the CEP to the dynamics in a chemostat, we see that due to the consistent flow of nutrients and continuous mixing, the environment is kept constant and the development of different niches due to spatial heterogeneity is not possible; therefore, it must be some form of inter- or intra-species interactions such as crowding, chemical signaling, cooperativity, or mutual inhibition that lead to any observed coexistence. Studying these interactions in simple chemostat systems gives us a better understanding of the factors that maintain the diversity in naturally occurring microbial consortia.

Natural consortia are often found to form *syntrophic* systems, where the microbes depend on each other for survival, either by the production of required metabolic substrates or by the maintenance of chemically advantageous conditions [54]. It is often observed that this syntrophic cooperation within microbial consortia increases their productivity and can allow the consortia to perform advanced functions that the microbial species are not capable of individually. These microbial interactions are known to be important in diverse areas including chronic medical infections (e.g. diabetic ulcers [21, 29]), biofuel synthesis (e.g. biodiesel production [44, 70]), environmental nutrient cycling (e.g. CO_2 sequestering, nitrification [8]), bioprocessing [60], and wastewater treatment [53, 57, 58].

A frequently observed syntrophic system is a *cross-feeding* chain where microbes work together to perform the sequential degradation of complex compounds like lingocellulosic material [54]. In these syntrophic cross-feeding systems a single substrate must be broken down in many steps, with one species catabolizing the available substrate and oxidizing it to produce a byproduct that the next species in the chain can consume. The intermediate byproducts in these systems are often found to be inhibitory. In this work we will consider the case where the intermediate byproduct inhibites growth. However, this more complicated system can be reduced to the case where there is no inhibition by taking the appropriate limit.

It has been observed experimentally that these syntrophic chain systems where the metabolic pathways are split among separate organisms (known as

'*microbial specialisation*' or a '*division of labor*') are more productive than a single organism with the equivalent metabolic capabilities [3, 67]. For example, if we compare a single organism that metabolizes $A \to B \to C$ to a pair of organisms that metabolize $A \to B$ (organism 1) and $B \to C$ (organism 2), experimental observation has found the pair of organisms to be more productive than the single organism. Productivity is defined here as total biomass production per unit of input A.

An example of this division of labor that has been found to evolve repeatedly in different experiments occurs when *E. coli* is grown on a glucose substrate. The original population of *E. coli* can fully metabolize glucose (glucose→acetate→CO_2 (TCA cycle)), but when grown on glucose for many generations the population splits into two main subpopulations: microbes that preferentially consume glucose and produce acetate (glucose→acetate) and microbes that preferentially consume acetate (acetate→CO_2) [50, 51, 64].

In this paper we use standard chemostat modeling techniques to investigate whether the division of labor (splitting the pathways into two separate organisms) alone is sufficient to explain the observed increase in biomass, and if not, what other changes may be required. It is important to note that in contrast to the past work which has investigated the evolution of such cross-feeding systems, we will not consider the two systems in direct competition, instead comparing the maximum biomass (productivity) of the systems in isolation. This is motivated by industrial applications where the total productivity of the consortia, which is usually proportional to the biomass, is of primary interest.

This type of system has been studied mathematically, and it can be shown that for n species in a simple syntrophic cross-feeding chain, there is a stable coexistence steady state [33, 46, 47, 48]. This simple system has been modified to include other forms of inhibition, external toxins, multiple substrates, and other forms of mutualism; in all cases, a stable, stationary, coexistence steady state is found [2, 5, 15, 31, 52]. Previous research has focused on proving the existence and stability of coexistence steady-states. There has been no investigation of the productivity of these syntrophic chain systems. Some recent work [10, 16, 45] investigated the evolution of cross-feeding in microbial populations and found that there are a wide range of parameter values for which cross-feeding is seen to evolve. The aim of these evolution studies was to identify conditions for stable coexisting syntrophic chain systems to evolve and outcompete equivalent monocultures. They did not explicitely investigate the productivity of the systems that are found to evolve.

In our initial model, we assume that the metabolic dynamics of the pathways do not change when being split into a separate microbes. In addition, we initially assume that the growth rate for the monoculture is a linear combination of the growth rates of the two pathways. This formulation allows us to obtain theoretical results and is effectively an upper bound on the growth rate of the monoculture microbe. Realistically, there are costs to utilizing both pathways at once for the monoculture, and there are changes that are known to occur to the metabolic pathway dynamics when the microbes specialise to a single substrate. For example, Pfeiffer and Bonhoeffer [45] theorize that the evolution

of cross-feeding could be due to the system minimizing the concentration of inhibitory intermediates and minimizing the concentration of enzymes it must produce, while maximising the rate of ATP-production. Another explanation comes from Johnson *et al.* [30] who find, by considering the biochemical conflicts which constrain the relationships between two metabolic processes, that the division of metabolic pathways could be advantageous as it allows microbes to focus on producing a smaller number of enzymes and optimizing a smaller subset of pathways.

By starting with the assumption of no adaptation for the specialists and the maximal growth rate for the monoculture, we get a strong theoretical result. Then, by varying the growth kinetics (growth rates and substrate affinities) and yields between the monoculture and the binary culture systems, we are able to use our model to test possible explanations for the observed increase in productivity and to quantitatively investigate what changes are required for the division of labor to be advantageous (increased biomass). Considering the specific example of *E. coli* grown on a glucose substrate [50, 51, 64], we use standard Monod kinetics and measured experimental parameters to determine the conditions under which the model results match the experimentally observed increase in biomass.

The main result of this work is a comparison of the biomass production of a single microbe with full metabolic capacity to a syntrophic consortium of two specialized microbes each with a unique subset of the full metabolic chain, where the intermediate byproduct may be inhibitory. We prove that the monoculture system will always have higher biomass production (i.e., higher productivity) if there are no changes to the growth kinetics or yield of the pathways between the two systems. In a specific example, we show that increasing the growth rates or substrate affinities of the consortial pathways, a change that might be expected due to specialisation, is not sufficient to generate the observed higher biomass production in the binary consortia. However, by varying the yields for the consortial pathways, higher biomass production can be achieved for the binary consortia relative to the monoculture. Yield changes are an expected result of microbial specialisation because utilizing a smaller number of specialized pathways leads to reduced energy requirements. This result provides evidence for the argument that an increase in efficiency (yields) is a key factor underlying the observed productivity benefit of microbial consortia. Additionally, the finding that changing yields can lead to higher biomass production through specialisation has important implications for industrial settings where higher biomass production is often highly desirable.

2. Model Construction

To investigate the effects of separating metabolic pathways, we will analyse the simplest case of a syntrophic chain where there are only two microbial species. For clarity we will use a specific example in developing our notation, in this case the metabolism of glucose by *E. coli*. To construct the model we assume that the metabolism of a single provided substrate (glucose, G)

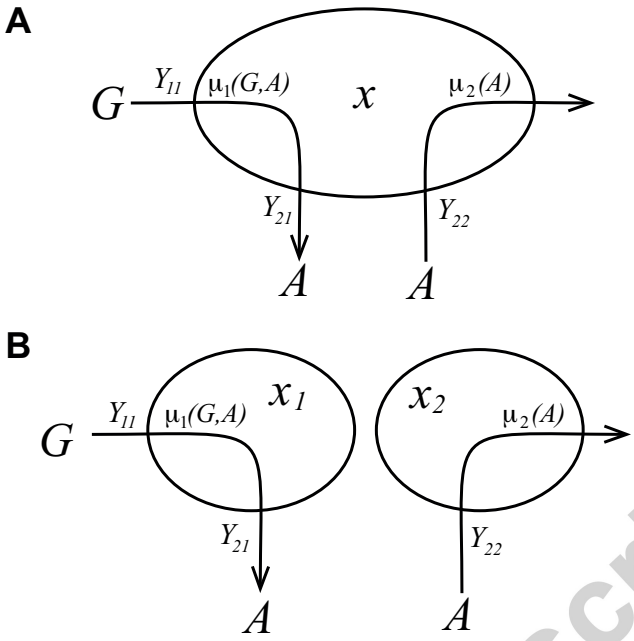

Figure 1: Diagram showing the metabolic pathways in (a) the monoculture system with the microbes x and (b) the binary culture system with the primary (glucose) consumer x_1 and the scavenger (acetate consumer) x_2, where G is the primary substrate (glucose) and A is the inhibitory intermediate substrate (acetate). The yields Y_{11} and Y_{22} fix the rates of biomass production per gram of substrate consumed, the yield Y_{21} is the ratio of biomass production to byproduct production, and the growth rates are given by the functions $\mu_1(G, A)$ and $\mu_2(A)$.

can be split into two pathways. The first step (pathway) takes substrate G and produces an intermediate by-product A (acetate), creating new biomass at a growth rate $\mu_1(G, A)$. The intermediate by-product acetate A serves as a substrate for the second step (pathway), which has a growth rate $\mu_2(A)$. As well as being a substrate, acetate lowers the pH and is detrimental to both metabolism pathways in the cell, which slows the growth rates μ_i and thus slows the uptake of substrate. The lower pH caused by acetate production could also increase the energy required for cell homeostasis, which would affect the yield parameters. We do not consider this effect here, as if yield did decrease at higher A values, this would further disadvantage the binary consortia, and thus would not qualitatively affect our results but would greatly complicate the analysis.

We will consider the situation where the microbes are grown in continuous culture (chemostat). We compare the total biomass produced in two different systems: a binary culture system where the two pathways are in two separate microbes, and a monoculture system where the pathways are combined into a single microbe. These two systems are shown in Figure 1. For the monoculture system, acetate that is produced through the first pathway is then available to be consumed through the second pathway. If the acetate consumption rate is

lower than the acetate production rate, acetate will accumulate in the system, see equations (4) and (7). In our model of the monoculture, we consider the case where acetate is consumed (metabolized) by the individual microbial cell that produced it, and the case where acetate is released from that microbe into the environment and then consumed by distinct microbes, to be equivalent. This is possible because this model does not include any cost involved in transporting acetate into or out of the cell. Including a cost for transporting acetate would disadvantage the binary consortia compared to the monoculture, and thus it would not qualitatively affect our results.

2.1. Model formulation

To model the dynamics in a chemostat we construct a system of ordinary differential equations (ODEs), following standard techniques [61], that describe the evolution over time of the microbial biomass and substrate concentrations. In both systems we will track the concentration of primary substrate, G and the concentration of the intermediate by-product, A.

In binary culture, the biomass of a microbe that consumes G and produces A to grow at rate $\mu_1(G, A)$ will be denoted by x_1, and the biomass of the second microbe that consumes A and grows at rate $\mu_2(A)$ will be x_2. For the binary chemostat this situation can be described by the following system of ordinary differential equations:

$$\frac{dx_1}{dt} = (\mu_1(G, A) - D)x_1, \tag{1}$$

$$\frac{dx_2}{dt} = (\mu_2(A) - D)x_2, \tag{2}$$

$$\frac{dG}{dt} = (G_{\text{in}} - G)D - \frac{\mu_1(G, A)}{Y_{11}}x_1, \tag{3}$$

$$\frac{dA}{dt} = -AD + \frac{\mu_1(G, A)}{Y_{21}}x_1 - \frac{\mu_2(A)}{Y_{22}}x_2, \tag{4}$$

where $D > 0$ is the dilution rate (with units $1/hr$, and $D = V/Q$ where V is the volume and Q is the volumetric flow rate) and $G_{\text{in}} > 0$ is the input concentration of primary substrate. The parameters D and G_{in} are set by experimental conditions. The yields, constants Y_{ij}, are determined by the stoichiometry of the metabolic pathways involved, which dictates the energy produced per unit of substrate consumed, and the proportion of energy produced that goes towards biomass production, which depends on additional factors including the energy required for cell homeostasis and for the production of enzymes. In this work we have chosen to define the yield terms Y_{11} and Y_{22} as the amount of biomass made by one unit of substrate, G and A respectively, and Y_{21} is the amount of biomass produced when one unit of intermediate substrate A is produced through the G-metabolism pathway. The parameter, $r = Y_{11}/Y_{21}$ defines the grams of the inhibitory intermediate substrate A produced per gram of primary substrate A consumed, and is fixed for a specific metabolic pathway.

To model the monoculture system, we assume that the two pathways are combined in a single microbe, whose biomass is represented by the variable x. The growth rate is assumed to be the sum of the metabolic pathways of the two microbes ($\mu_{WT} = \mu_1(G, A) + \mu_2(A)$). This provides the maximal possible growth rate for the monoculture, without making further assumptions on whether monoculture can actually use this potential. In reality, using both pathways concurrently comes at a cost, as microbes have finite resources for the transport of nutrients into the cell, and the production of enzymes. We will later (Section 4.3) consider modelling the monoculture growth rate as a convex combination of the pathways ($\bar{\mu}_{WT} = \beta f(G)I(A) + (1 - \beta)m(A)$). However, we start the linear combination ($\mu_{WT} = \mu_1(G, A) + \mu_2(A)$), which is the upper bound for the wildtype growth rate, in order to be able to obtain theoretical results. This gives the system of rate equations for the monoculture system:

$$x' = [\mu_1(G, A) + \mu_2(A) - D]\, x, \tag{5}$$

$$G' = (G_{\text{in}} - G)D - \frac{\mu_1(G, A)}{Y_{11}}\, x, \tag{6}$$

$$A' = -AD + \left[\frac{\mu_1(G, A)}{Y_{21}} - \frac{\mu_2(A)}{Y_{22}}\right] x. \tag{7}$$

In this formulation we assume that there is no change in pathway efficiency (yield), growth rate, substrate affinity, or inhibition when the pathways are split into two separate microbes, thus the functions and parameters for the monoculture system (5)-(7) are identical to those in the binary culture system (1)-(4).

In this work we will assume that the inhibition by A on the first pathway is non-competitive, so that the growth rate of pathway 1 can be described by $\mu_1(G, A) = f(G)I(A)$, where the function $f(G)$ describes the growth of x_1 on G and the function $I(A)$ describes the inhibition of x_1 by A. The growth of x_2 due to the consumption of A we describe by the function $\mu_2(A) = m(A)$, where $m(A)$ increases at low A values but decreases when A gets too high.

2.2. Model non-dimensionalization

In order to simplify the calculations, we non-dimensionalize the original system using the scalings:

$$\hat{x} = \frac{x}{G_{in}Y_{11}}\,,\ \hat{x_1} = \frac{x_1}{G_{in}Y_{11}}\,,\ \hat{x_2} = \frac{x_2}{G_{in}Y_{11}}\,,$$

$$\hat{G} = \frac{G}{G_{in}}\,,\ \hat{A} = \frac{AY_{21}}{G_{in}Y_{11}}\,,\ \hat{t} = tD\,,\ \gamma = \frac{Y_{21}}{Y_{22}}\,. \tag{8}$$

This gives us the dimensionless variables $(\hat{x_1}, \hat{x_2}, \hat{G}, \hat{A})$ for the binary culture and $(\hat{x}, \hat{G}, \hat{A})$ for the monoculture. Both systems of equations depend upon the new dimensionless time variable $\hat{t}$, and the only remaining parameter in the system is the dimensionless parameter γ.

Removing the hats for convenience and making the substitution $\mu_1(G,A) = f(G)I(A)$, $\mu_2(A) = m(A)$, gives us a dimensionless version of the binary culture system (equations (1)-(4))

$$\begin{aligned} x_1' &= (f(G)I(A) - 1)x_1, \\ x_2' &= (m(A) - 1)x_2, \\ G' &= 1 - G - f(G)I(A)x_1, \\ A' &= -A + f(G)I(A)x_1 - \gamma\, m(A)x_2, \end{aligned} \tag{9}$$

and a dimensionless version monoculture system (equations (5)-(7))

$$\begin{aligned} x' &= [f(G)I(A) + m(A) - 1]\, x, \\ G' &= 1 - G - f(G)I(A)\, x, \\ A' &= -A + [f(G)I(A) - \gamma\, m(A)]\, x. \end{aligned} \tag{10}$$

2.3. Model assumptions

Before we describe our main result, it is important to specify our assumptions on the functions and parameters in the model (in the dimensionless setting).

A1. The functions $f(G)$, $I(A)$ and $m(A)$ are the same in both models, i.e. that the separation of the pathways does not modify the metabolic dynamics.

A2. The function $f(G)$ is a monotonically increasing function of substrate concentration, G, with limiting rate, $\mu_{1,max}$ (see Figure 2(a)). The properties of $f(G)$ are:

$$\begin{aligned} f(0) &= 0, \\ \lim_{G\to\infty} f(G) &= \mu_{1,max}, \\ \frac{df(G)}{dG} &> 0 \quad \text{for } G \geq 0, \\ \lim_{G\to\infty} \frac{df(G)}{dG} &= 0. \end{aligned} \tag{11}$$

These conditions on $f(G)$ are readily satisfied by an increasing Hill function $\mu_{1,max}G^n/(k^n + G^n)$ for any n.

A3. The function I describes the inhibition of the G-metabolism pathway by the intermediate substrate A (see Figure 2(b)). The properties of $I(A)$ are:

$$\begin{aligned} I(0) &= 1, \\ I(A) &> 0 \quad \text{for } A \geq 0, \\ lim_{A\to\infty} I(A) &= 0, \\ \frac{\partial I(A)}{\partial A} &< 0 \quad \text{for } A > 0. \end{aligned} \tag{12}$$

These conditions on $I(A)$ are satisfied by a decreasing Hill function $k^n/(k^n + A^n)$ for any n.

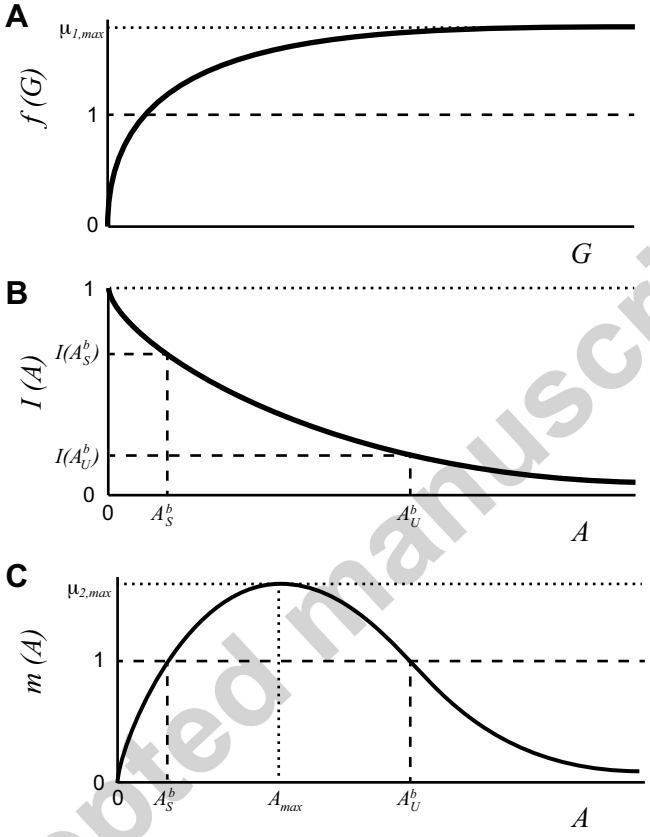

Figure 2: Qualitative sketch of the growth and inhibition functions: (a) $f(G)$, (b) $I(A)$, and (c) $m(A)$ in nondimensional variables. The solutions to the equation $m(A) = 1$, A_S^b and A_U^b, are shown in panels (b) and (c).

A4. The function $m(A)$ describes the growth rate on the inhibitory substrate (A) (see Figure 2(c)). $m(A)$ has the following properties:

$$\begin{aligned} m(0) &= 0, \\ \lim_{A\to\infty} m(A) &= 0, \\ max(m(A)) &= m(A_{max}) = \mu_{2,max}, \\ \frac{dm(A)}{dA} &> 0 \quad \text{for } 0 \le A \le A_{max}, \\ \frac{dm(A)}{dA} &= 0 \quad \text{at } A = A_{max}, \\ \frac{dm(A)}{dA} &\le 0 \quad \text{for } A_{max} \le A, \\ \lim_{A\to\infty} \frac{dm(A)}{dA} &= 0. \end{aligned} \tag{13}$$

These conditions on $m(A)$ are satisfied by commonly used substrate-inhibition functions [24].

A5. We consider the case where the growth rates of each microbe are sufficiently large that they can survive at the chosen dilution rate; i.e.,

$$\begin{aligned} \mu_{1,max} &> 1, \\ \mu_{2,max} &> 1. \end{aligned}$$

For $\mu_{2,max} > 1$ the equation $m(A) = 1$ has two solutions, which we define as A_S^b and A_U^b, where $A_S^b < A_U^b$.

A6. We consider the case where the substrate inflow is in excess, by which we mean $f(G_{\text{in}}) \approx \mu_{1,\max}$ and consequently, $f(G_{\text{in}}) > D$ (in the original variables). These conditions correspond to $f(1) \approx \mu_{1,\max}$ and $f(1) > 1$ in the dimensionless setting.

We use the product form of the function $\mu_1(G, A) = f(G)I(A)$ since it captures the growth and non-competitive inhibition of pathway 1 and simplifies the analysis. However, a more general function $\mu_1(G, A)$ with the properties $\frac{\partial \mu_1(G,A)}{\partial G} > 0$ for all $G > 0$ and $\frac{\partial \mu_1(G,A)}{\partial A} < 0$ for all $A > 0$ may be used if inhibition is known to be competitive.

3. Main results

In this section we present our main result, the proof of which can be found in the Appendix. The implications of this technical result are then demonstrated with an example from a realistic situation in the following sections.

3.1. Binary culture system equilibria and stability

For the binary culture (9) we differentiate between three different types of equilibrium points: *trivial* equilibria where $x_1 = 0, x_2 = 0$, *boundary* equilibria where $x_1 \neq 0, x_2 = 0$ (note there are no $x_1 = 0, x_2 \neq 0$ equilibria, as G is the only substrate provided to the chemostat system), and *co-existence* equilibria where $x_1 \neq 0, x_2 \neq 0$. We consider only equilibria in the positive cone $(x_1, x_2, G, A) \in \mathbb{R}^4_+$.

Theorem 1. *Given Assumptions [A1.]-[A6.] in Section 2.3, the binary culture system (9) has the following equilibria:*

a. *There exists a trivial equilibrium when there are no microbes in the system at* $(x_1, x_2, G, A) = (0, 0, 1, 0)$*, for all functions satisfying [A2.]-[A4.]. This trivial equilibrium point is an unstable saddle for all parameter values satisfying [A5.]-[A6.].*

b. *There exists a boundary equilibrium point, where only x_1 survives, at* $(x_1^1, x_2^1, G^1, A^1) = (1 - G^1, 0, G^1, 1 - G^1)$*, where G^1 is implicitly defined by* $f(G^1)I(1 - G^1) = 1$*. The stability depends on the specific functions and parameters.*

c. *We define a value $A = A^b_{\text{crit}}$, where A^b_{crit} is implicitly defined by* $I(A^b_{\text{crit}}) = 1/\mu_{1,max}$*.*

(i) *If $A^b_{\text{crit}} < A^b_S$, or if $A^b_S < A^b_{\text{crit}}$ but $G^b_S + A^b_S > 1$, there are no co-existence equilibria. The boundary equilibrium point is a stable node.*

(ii) *If $A^b_S < A^b_{\text{crit}} < A^b_U$, and $G^b_S + A^b_S < 1$, or if $A^b_U < A^b_{\text{crit}}$, and $G^b_S + A^b_S < 1$, but $1 < G^b_U + A^b_U$, there is a single, stable, co-existence equilibrium point $S := (x^b_{1,S}, x^b_{2,S}, G^b_S, A^b_S)$. The boundary equilibrium point is an unstable saddle.*

(iii) *If $A^b_U < A^b_{\text{crit}}$, and $G^b_U + A^b_U < 1$, there are two co-existence ($x_1 \neq 0, x_2 \neq 0$) equilibria, $S := (x^b_{1,S}, x^b_{2,S}, G^b_S, A^b_S)$ and $U := (x^b_{1,U}, x^b_{2,U}, G^b_U, A^b_U)$. The point U is an unstable saddle, and the point S is a stable node. The boundary equilibrium point is a stable node.*

Proof. A

Remark 1. The conditions related to A^b_{crit} ensure that the equation $f(G)I(A) = 1$ has a solution for the given A^b value. The conditions $G^b + A^b < 1$ ensure that the equilibrium biomass values (x_1 and x_2) are strictly positive; if $G^b + A^b > 1$ then $x^b_{2,U} < 0$ and the equilibrium point is non-physical.

Remark 2. Note that in case (iii) of Theorem 1c. the system is bistable, with the stable manifold of the saddle point U forming a separatrix that separates the basins of attraction of the two stable equilibria, S and the boundary equilibrium point.

3.2. Monoculture system equilibria and stability

For the monoculture system (10), there are two types of equilibria: *trivial* equilibria where $x = 0$ and *non-trivial* equilibria where $x \neq 0$.

Theorem 2. *Given Assumptions [A1.]-[A6.] in Section 2.3, the monoculture system (10) has the following equilibria:*

a. *There exists a trivial equilibrium point at $(x, G, A) = (0, 1, 0)$, which is an unstable saddle.*

b. *There are $2n + 1$ non-trivial ($x \neq 0$) equilibria $E_i := (x_i^m, G_i^m, A_i^m)$ in the region $A < A_S^b$, where $n \geq 0$, ordered by increasing A_i^m. If there is a unique internal equilibrium ($n = 0$) this equilibrium point is a stable node. If there are multiple internal equilibria, the odd equilibria ($i = 1, 3, .., 2n+1$) are stable nodes, and the even equilibria ($i = 2, 4, .., 2n$) are unstable saddles.*

c. *If the curve $G = 1 - A/(1 + \gamma - \gamma/(1 - m(A)))$ intersects the curve $f(G)I(A) + m(A) = 1$, in the region $A > A_U^b$, then there is an even number of equilibria $K_j, j = 1, \ldots, 2m$. If we order these equilibria by increasing value of A, then the odd equilibria are saddles and even equilibria are nodes.*
These curves can only intersect if $m(A) = 1 - \gamma/(1 + \gamma - A)$ has more than one solution. This condition is illustrated in Figure 3. If

$$\mu_{1,\max} I(A_2^v) < \frac{\gamma}{1+\gamma}, \tag{14}$$

these equilibria do not exist, where A_2^v is the upper solution of $m(A) = 1/(1 + \gamma)$. This condition is illustrated in Figure 3.

Proof. B

Remark 3. The equilibria K_j only exist in specific circumstances when the monoculture growth is less inhibited by acetate than the acetate consuming specialist (see (14) for exact statement), while at least one lower equilibrium E_i exists for all parameter values satisfying [A1.]-[A6.]. The high A (low biomass) stable equilibria, when they exist, have a small basin of attraction, which is characterized by high levels of acetate and low levels of glucose. Only initial conditions with high initial acetate and low glucose can lead to a monoculture that evolves to such stable equilibrium. For this reason, we do not consider these equilibria in the results below.

3.3. Biomass comparison

We wish to compare the productivity of the binary culture and monoculture systems, using their total biomass as a measure of productivity.

The biomass for the binary system is largest at the stable co-existence equilibrium point S, since it can be easily shown that $x_{1,S}^b + x_{2,S}^b > x_1^1$ (see Appendix

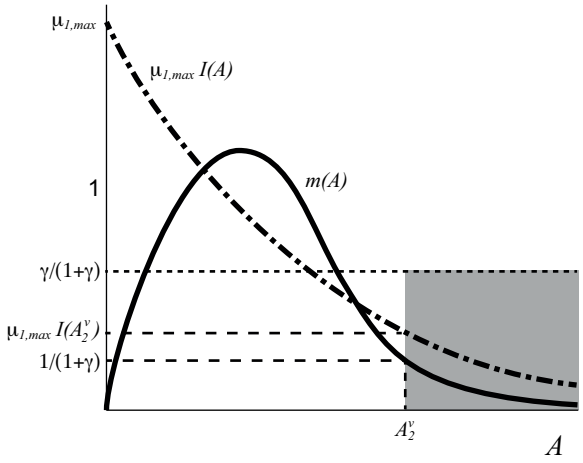

Figure 3: Qualitative sketch of the curves $m(A)$ (solid black curve) and $\mu_{1,\max} I(A)$ (dot-dash black curve) that satisfy the sufficient condition in Theorem 2c. ruling out the upper monoculture equilibria. The curve $\mu_{1,\max} I(A)$ lies in the shaded region defined by the value $m(A_2^v)$, where A_2^v is the upper solution of $m(A) = 1/(1+\gamma)$.

C). The monoculture system has (at least) one stable non-trivial equilibrium point E_i, with high biomass. Since we do not consider the possible upper equilibria K_j with low biomass to be physical, we will compare the biomass at the binary system equilibrium S with an arbitrary monoculture equilibrium E_i.

Theorem 3. *Given Assumptions [A1.]-[A6.] in Section 2.3, and the existence of at least one (stable) co-existence equilibrium point, S, in the binary system (conditions in Theorem 1(c.). Then the biomass of the monoculture, x_i^m, at any of the stable non-trivial equilibrium points E_i for $i = 1, 3, ...2n+1$ is always higher than the total biomass of the binary culture system $x_{1,S}^b + x_{2,S}^b$ at its stable co-existence equilibrium point S:*

$$x_i^m > x_{1,S}^b + x_{2,S}^b.$$

Proof. C
Outline of the proof. We show in C that the monoculture biomass is given by

$$x^m = \left(1 + \frac{1}{\gamma}\right)(1 - G^m) - \frac{A^m}{\gamma}\,, \tag{15}$$

and the combined biomass of the binary culture is

$$x_{tot}^b = x_{1,S}^b + x_{2,S}^b = \left(1 + \frac{1}{\gamma}\right)(1 - G_S^b) - \frac{A_S^b}{\gamma}\,. \tag{16}$$

We can also show that for all E_i monoculture equilibria:

$$G_S^b > G_i^m \quad \text{and} \quad A_S^b > A_i^m\,. \tag{17}$$

Thus,

$$\left(1+\frac{1}{\gamma}\right)(1-G_S^b)-\frac{A_S^b}{\gamma}<\left(1+\frac{1}{\gamma}\right)(1-G^m)-\frac{A^m}{\gamma}$$

and the biomass of the binary culture is always less than the biomass of the monoculture:

$$x_{1,S}^b+x_{2,S}^b<x^m.$$

Remark 4. If there are no upper equilibria in the monoculture, E_i for $i = 1, 3, ...2n + 1$ are the only stable equilibrium points of the system, and the monoculture biomass will always be higher than the total biomass of the binary culture, for all initial conditions $(G, A) \in \mathbb{R}_+^2$.

4. Effect of modifications to the model on relative biomass

In chemostat experiments, a binary culture of the type analysed here shows a biomass increase of around 20% over a wild-type monoculture system [3]. As we have shown in Theorem 3, under our assumptions the monoculture system always has a higher biomass. Clearly this means that one or more of the assumptions that we make in Section 2 are incorrect. This is useful, as by examining the assumptions we made, we can investigate which of the effects that we did not include are most relevant.

One of the assumptions we made in formulating the initial model is that there is no change in the growth dynamics or yields of the metabolic pathways when the microbes specialise to a single substrate. However, as discussed already, there is evidence that the growth dynamics and pathway efficiencies will change, and we will investigate the effects of incorporating these changes in this section.

4.1. Increasing the growth rates in the binary culture system

Experiments have observed that growing *E. coli* on a single nutrient source can increase its growth rate ∼15-20% [12, 28, 3], as the microbe adapts to the single nutrient and can up regulate the transport for that substrate [42] and down regulate the transport for the pathways it is not using (catabolite repression [13, 35]). We can incorporate the effect of increasing the growth rate of the species in the binary culture system by introducing multiplicative parameters α_1 and α_2 in front of growth rates $f(G)$ and $m(A)$, thus making the replacements:

$$f(G)\to\alpha_1 f(G)\,,\qquad m(A)\to\alpha_2 m(A). \tag{18}$$

Note that this increases the growth rates at all concentrations of G and A, not just for high growth regions of G or A. For the original systems (with no change in growth rate) we have $\alpha_1 = 1$, $\alpha_2 = 1$. To simulate an increase in growth rate when the metabolic pathways are split up we simply choose $\alpha_1, \alpha_2 > 1$ in the binary culture system.

Increasing α_1 decreases $G_S^b \to 0$, while increasing α_2 in the binary culture moves $A_S^b \to 0$, which in turn decreases G_S^b (bounded below by G_0). We find

that it is always possible to get higher biomass for the binary culture than the monoculture ($G_S^b < G^m, A_S^b < A^m$) if there are no bounds on the increases for both α_1 and α_2. If we can only vary one pathway's growth rate, i.e., keeping $\alpha_1 = 1$ or $\alpha_2 = 1$, then it is not always possible to get higher biomass in the binary culture. Whether or not it is possible to surpass the monoculture biomass, and the increases in growth rate required, will depend on the specific functions and parameters for the system of interest.

4.2. Increasing the substrate affinity in the binary culture system

When growing on a single carbon source, it has been found that some microbes, including *E. coli*, can increase their affinity when the concentration of the substrate remains low for an extended period of time [27, 59]. This is thought to be achieved through up-regulating higher affinity transporters [18]. Decreasing K_G, moves $G_S^b \to 0$, while decreasing K_A moves $A_S^b \to 0$, which in turn decreases G_S^b (bounded below by G_0). This matches the effects of increasing the growth rates by a factor α_1 or α_2 in Section 4.1. We can explain this mathematically as follows: in the region where G (or A) is low, increasing the substrate affinity acts to increase the growth rate for that G (or A) value. By considering $f(G)$ at low G, we find that $f(G) \approx \frac{\mu_{1,\max}}{K_G} G$ for small G, so increasing $\mu_{1,\max}$ or decreasing K_G by the same factor should have the same effect.

4.3. Varying the form of the monoculture growth rate

It could be argued that the monoculture out-performs the binary culture in our formulation due to the way we have described the monoculture growth rate ($\mu_{WT}(G, A) = f(G)I(A) + m(A)$). In this formulation we are assuming that the microbe can use both pathways concurrently, with both functioning at their maximal rates for the specific G and A. This acts as an upper bound on the maximal possible growth rate for the monoculture. In reality, there are limitations due to the transport of nutrients into the cell and the energy required for the synthesis and maintenance of metabolic enzymes. It has been observed experimentally that often a microbe preferentially consumes the substrate sustaining the higher growth rate (catabolite repression). In this process, the synthesis of enzymes required for alternate pathway is down-regulated, which would decrease the maximal growth rate of these other pathways. If we assume that the cell must choose to allocate resources between the two pathways, we can incorporate this into our model by making the monoculture's growth rate a convex combination of the two pathways' growth rates:

$$\bar{\mu}_{WT} = \beta f(G)I(A) + (1 - \beta)m(A). \tag{19}$$

Where β could be some function of the relative growth rates of the two pathways at the given G and A concentrations, following [1, 13, 35].

According to catabolite repression the microbe will only consume the preferred substrate. However, if the intermediate substrate is inhibitory there is

often a 'switch' that overrides this effect at high A to consume the excess intermediate substrate and decrease the inhibitory effects [68]. In our model, we could incorporate this by using (19), with β being a function of A, switching to low β (increased A consumption) when A reached a critical value, even in the presence of high G.

Using $\bar{\mu}_{WT}$, we cannot get theoretical results for the relative productivy of the monoculture and binary culture systems in general, as the biomass will depend on the specific situation and the β values (or functions) chosen. However, we can easily show that for sufficiently high or low β the binary culture system would now out-perform the monoculture system:

- At $\beta = 1$, the monoculture growth rate is given solely by $f(G)I(A)$, which is the equivalent of the binary culture system with $x_2 = 0$. In Appendix C we showed that this x_1-only equilibrium point has a lower biomass than the binary culture system coexistence equilibrium point, thus the binary culture outperforms the monoculture.

- As $\beta \to 0$, the monoculture growth rate is increasingly dependent on the second pathway, $m(A)$, which consumes exclusively acetate A. Since glucose G is the only substrate provided to the chemostat, we expect that the monoculture will not survive.

Based on optimal foraging theory and experiments, it is reasonable to assume that *E. coli* feeding on multiple substrates would allocate resources to pathways such that the growth rate is maximized [1, 13, 35], and this is indeed what is found with catabolite repression. In a chemostat at equilibrium, the growth rate is always fixed to the dilution rate D, so we cannot determine the optimum β value at equilibrium. One option could be to first find the β values required for the monoculture system to have lower biomass (for a given system), then to use the optimal foraging arguments to determine whether these β values are realistic by looking at the ratio of μ_1 to μ_2 for the given G and A values. Another option would be to look at what β value maximizes biomass, and consider whether this leads to higher biomass in the monoculture than the binary culture, and whether this is a reasonable β value. We will consider both in section 5.2.3 for the specific example of *E. coli* growing on glucose.

4.4. Increasing the efficiencies (yields) in the binary culture system

The yield terms Y_{11} and Y_{22} describe the amount of biomass produced per unit of substrate consumed, and are a measure of the microbe's efficiency. The yields are determined by only two factors: how much energy the pathway can produce (given by the stoichiometry of the pathway), and how much of the energy produced is allocated to biomass production.

There are many ways that microbes can adapt to optimize their productivity, but only some of these will increase the yield terms in our formulation. For example, it is observed that when provided with multiple substrates, cells will consume the most productive substrate preferentially (also known as catabolite repression). In this way, the microbes are utilizing the most efficient pathways

and thus increasing their efficiency. In our model the binary culture microbes only have one substrate, and thus catabolite repression will not affect their dynamics. In the monoculture, catabolite repression would lead to the most efficient pathways being prioritised. This increase in resources would increase the substrate uptake and growth rate of the preferred pathway, and could be incorporated into our model through changing the parameter β as described above, where $\beta = 1$ describes consumption of the primary substrate only. However, as the stoichiometry of the pathways does not change, this effect would not directly change Y_{11} or Y_{22} in our model.

In order to increase the yield, a microbe must reduce the energy that is required for functions other than biomass production, such as cell homeostasis and enzyme production. Microbes growing on a single source are thought to down-regulate the production of enzymes for the metabolism of other substrates [30]. Since the synthesis and maintenance of metabolic enzymes requires energy, if a microbe can reduced its net enzyme production in this way, this would reduce the energy required and its yield would increase. Thus it is possible that by specialising to a single substrate, the yields Y_{11} and Y_{22} would increase.

Another factor that could affect the energy requirements, is the cost of transporting substrates into the cell. So far we have not included this cost. If we were to include the cost of transporting the primary substrate G into the cell, this would decrease the term Y_{11} in both binary and monoculture systems equally. Including the cost of transporting the inhibitory intermediate substrate A into the cell, would decrease Y_{22}. The binary culture needs to transport all of the consumed A into the scavenger specialist x_2, whereas the monoculture can metabolize intracellular A as it is produced, as well as transporting A into the cell, thus deflecting some of this cost. Therefore, Y_{22} would decrease more in the binary culture than in the monoculture system.

Examining the equations for steady-state biomass we find that changing Y_{11} does not affect the nondimensionalized binary biomass, but from equation (8) it will affect the actual (dimensional) biomass. The total biomass of the binary culture increases when Y_{11} increases (the G-metabolism pathway becomes more efficient). When Y_{22} increases (the A-metabolism pathway becomes more efficient), or when Y_{21} decreases (the amount of inhibitory metabolite produced increases), γ decreases, which will increase the total biomass of the binary culture. As discussed in Section 2.1,the ratio $r = Y_{11}/Y_{21}$, which describes the grams of the inhibitory intermediate substrate produced per gram of primary substrate consumed, is fixed for a specific metabolic pathway. Therefore, varying Y_{21} or Y_{11} independently is not realistic, and in the latter analysis we will vary Y_{11} and Y_{21} together, keeping r constant. When making increases to Y_{11} or Y_{22} we must keep in mind that there is an upper bound on the yield terms that given by the stoichiometry of the utilized metabolic pathway. Whether the yield increase required to match the observed increase in biomass for the binary culture is above that bound will depend on the system of interest.

4.5. Varying G_{in} and D

Some earlier work has found that the binary culture is favoured over a monoculture for certain substrate inflow concentrations G_{in} or dilution rates D [10, 45]. However, we find that for all G_{in} and D, satisfying assumptions [A5.] and [A6.], the monoculture has higher biomass than the binary culture. That being said, the difference in total biomass between the two systems will vary as G_{in} and D change, so there may be some experimental conditions where the binary culture is less disadvantaged, and where the aforementioned modifications would be more effective.

5. Specific example using Monod kinetics and typical values for *E. coli*

In this section, the results of this paper will be applied to the specific example of *E. coli* growing on glucose as the sole carbon source. Experimentally observed parameters for *E. coli* growth on glucose or acetate are summarized in Table 1. In the majority of the literature, *E. coli* were grown in aerobic conditions in which both pathways would be utilized. This will lead to overestimation of the parameters: $\mu_{1,\max}$, Y_{11}, Y_{21}, K_{IP}, and underestimation of the parameter r.

Parameter	Experimental values
Maximum growth rate on glucose[a] (h^{-1})	0.43-0.49 [b] [3], 0.57 [7], 0.43 (anaerobic) [7], 0.76 [11], 0.53 [17], 0.39 [20], 1.12 [23], 0.91 [32], 0.77 [40], 0.57 [43], 0.92 [59], 0.55-1.23 [59], 0.68 [65], 0.43 (anaerobic) [65], 0.54-0.55 [69]
Half-saturation glucose concentration[a] (mg/L)	7.2 [11], 0.04-180 [18], 100 [23], 4 [32], 0.68 [40], 0.0072 [59], 0.0053-99 [59], 50 [69]
Acetate product inhibition constant[a] (g/L)	4 [23], 4-5 [69], 9 [69]
Maximum growth rate on acetate (h^{-1})	0.11-0.15 [c] [3], 0.31 [12], 0.19 [23], 0.33 [42], 0.22 [43], 0.05 [69], 0.06-0.08 [69]
Half-saturation acetate concentration (g/L)	0.4 [23], 0.05 [69]
Acetate substrate inhibition constant (g/L)	3.8 [23]
Biomass yield (gBiomass/gGlucose consumed)[a]	0.23 [3], 0.26 [7], 0.18 (anaerobic) [7], 0.3 [17], 0.30 [20], 0.43 [32], 0.50 [43], 0.36 [65], 0.13 (anaerobic) [65], 0.52 [69], 0.49-0.51 [69], 0.15 (anaerobic) [69]
Acetate yield (gBiomass/gAcetate produced)[a]	0.4 [23], 0.3-0.9 [32]
Ratio (gAcetate produced/gGlucose consumed)[a]	0.25 [17], 0.38 [32]
Biomass yield (gBiomass/gAcetate consumed)	0.38 [12], 0.21-0.30 [43], 0.4 [69]

Table 1: Typical parameter values for *E. Coli* grown on glucose or acetate as the carbon source. See Table 4 for further details of the strains used and the specific experimental conditions. [a] the growth and yield of wildtype *E. coli* on glucose includes contributions from the acetate metabolism pathway, except in anaerobic conditions. [b]growth rate of mutant with acetate consumption pathway knocked out. [c]growth rate of mutant with glucose consumption pathway knocked out.

We can quantify the discrepancy between the actual yield of each pathway and the reported yield in wild-type aerobic conditions. If we assume that the

growth rate from the first (anaerobic) pathway is given by μ_1 and the growth from the aerobic metabolism of acetate (acetyl CoA) is given by μ_2, then the discrepancy between the actual yield of each pathway and the reported yield in wild-type aerobic conditions will be:

- The reported yield Y_{11}^{WT} (gBiomass/gGlucose consumed) will be overestimate by $Y_{11}^{WT} = Y_{11}(\mu_1 + \mu_2)/\mu_1$.
- The reported acetate production yield Y_{21}^{WT} (gBiomass/gAcetate produced) will be overestimated by $Y_{21}^{WT} = Y_{21}(\mu_1 + \mu_2)/(\mu_1 - \gamma\mu_2)$.
- The observed ratio r^{WT} (gAcetate produced/gGlucose consumed) will be underestimated by $r^{WT} = r(1 - \gamma\mu_2/\mu_1)$.

From the equation for Y_{11}^{WT} it can be seen that if $\mu_2 = 0$ (i.e. there is no metabolism of acetate, which occurs in anaerobic conditions), then $Y_{11}^{WT} = Y_{11}$. Thus, in order to estimate the parameters of just the first pathway ($\max f(G)$ and Y_{11}), we use the yield and growth parameters from anaerobic experiments [7, 65, 69]. To estimate Y_{21} we use the ratio $r = 0.667$ determined by the reaction stoichiometry and calculate $Y_{21} = Y_{11}/r$. Substituting reasonable values for growth rates, we find that our choice of parameters leads to observed Y_{21}^{WT} r^{WT} that match experimental data (Table 1). The observed growth and yield parameters for *E. coli* grown on acetate as the sole carbon source provide good estimates for $\max(m(A))$ and Y_{22}. The chosen yields are given in Table 2.

Parameter	Selected value	Notes
Y_{11}	0.152	from anaerobic growth experiments
$r = Y_{11}/Y_{21}$	0.667	reaction stoichiometry
Y_{21}	0.227	calculated, $Y_{21} = Y_{11}/r$
Y_{22}	0.400	

Table 2: Selected yield values for monoculture and binary culture systems.

It is important to note that for the yield terms Y_{11} and Y_{22}, which are the grams of biomass produced when one gram of substrate is consumed, only some of the energy from the the substrate metabolism will go towards biomass synthesis. Depending on the efficiency of the pathway, the energy produced per gram of substrate will vary, and the energy required for cell homeostasis (i.e. not available for biomass production) also varies. Estimates for the ratio of energy produced that goes towards biomass production and the efficiencies of the pathways used vary depending on the *E. coli* strain and the environmental conditions [6, 25]. We choose to use measured values for the total yield from the literature. These yields could vary with strain and condition, and we will consider this in Section 5.3.2. In all cases the yields are bounded above by the stoichiometry of the most efficient biomass production pathways assuming zero energy required for cell homeostasis, and our choices for yield parameters are below this bound and consistent with experimental findings.

To fit growth parameters, we must choose specific functions for $f(G)$, $I(A)$, and $m(A)$. Here we select Monod type kinetics for the growth and inhibition functions:

$$f(G) = \mu_{1,\max}\frac{G}{G + K_{\mathrm{G}}}, \tag{20}$$

$$I(A) = \frac{K_{\mathrm{IP}}}{K_{\mathrm{IP}} + A}, \tag{21}$$

$$m(A) = \mu_{2,\max}\frac{A}{A + K_{\mathrm{A}} + \frac{A^2}{K_{\mathrm{IS}}}}. \tag{22}$$

which satisfy assumptions [A2.]-[A4.] and are found to be appropriate for describing growth and inhibition rates of *E. coli* in chemostats or batch growth. With the exception of the half-saturation of glucose, K_G, experimental findings (Table 1) are reasonably consistent and the chosen parameters for these functions are given in Table 3.

Parameter	Selected value	Notes
$\mu_{1,\max}$	$0.6\mathrm{h}^{-1}$	$\max(f(G)) = 0.6\mathrm{h}^{-1}$
K_{G}	0.05g/L	
K_{IP}	0.5g/L	
$\mu_{2,\max}$	$0.8\mathrm{h}^{-1}$	$\max(m(A)) = 0.2\mathrm{h}^{-1}$
K_{A}	1.5g/L	half-saturation at $A = 0.23$g/L
K_{IS}	0.7 g/L	inhibited to half maximum at $A = 4.6$g/L
D	$0.1\ \mathrm{h}^{-1}$	chosen to prevent wash-out
G_{in}	10g/L	chosen to ensure excess substrate

Table 3: Selected parameter values for growth and inhibition functions given in equations (20), (21), (22), dilution rates, and substrate inflow concentrations.

At low glucose concentrations it is known that glucose affinity increases [18, 27], and the parameter K_G varies from O(0.01) to O(100) mg/L (Table 4) through the upregulation of higher affinity (and often slower or more energy intensive) pathways. In our model, K_G is a fixed parameter, and to demonstrate the results of this paper we choose an intermediate K_G value (see Table 3). This choice does not affect our result, as for equal substrate affinities the monoculture will outperform the binary culture for any choice of K_G (Theorem 3). We will investigate the effect of varying the glucose affinities between the monoculture and binary culture in Section 5.2.2. However, as increases in glucose affinity are found to depend mostly on the growth conditions, we would expect any increase in glucose affinity (K_G) to affect both the monoculture and the binary culture similarly.

In *E. coli* there are two pathways for acetate assimilation: the *phosphotransacetylase-acetate kinase* (*PTA-ACKA*) pathway and the *acetyl-CoA synthetase (acs)* pathway. The *PTA-ACKA* pathway has lower substrate affinity, with $K_m \approx 0.4 - 0.6$g/L [4, 68], but is more efficient requiring only one ATP for acetate assimilation. The *PTA-ACKA* pathway is found to be active until acetate gets to

low concentrations ($A \ll 0.15$g/L) [34]. In contrast, the *acs* pathway has higher substrate affinity, with $K_m \approx 0.01$g/L [4, 68], but is more energy intensive, requiring two ATP for acetate assimilation. Kumari et al. [34] find that both pathways are required for optimal growth on acetate across a range of concentrations, with the *acs* pathway being required for $A < 0.6$g/L and the *PTA-ACKA* pathway being required for $A > 1.5$g/L.

In our model, we use a single function $m(A)$ and single yield term Y_{22} to describes the growth kinetics and efficiency of growth on acetate; we do not include the two pathways separately. We choose growth parameters $\mu_{2,\max}$, K_A, and K_{IS} that match the experimentally observed growth in chemostat cultures which are utilizing both pathways. For example, the combined growth kinetics has a substrate affinity of $K_m = 0.23$g/L which is midway between the K_m values of each pathway. We will investigate the effect of varying the acetate affinities between the monoculture and binary culture in Section 5.2.2.

The yield parameter Y_{22} is fixed, so we have chosen $Y_{22} = 0.4$ which is at the lower end of the yields observed across a range of growth conditions [32]. This is because we find that in our model acetate concentrations stay low and the yield will be determined predominantly by the lower efficiency, higher affinity *acs* pathway.

The dilution rate D and glucose inflow concentration G_{in} are set by experimental conditions. We must select a dilution rate that satisfies non wash-out conditions (from assumption [A6.]: $\max(m(A)) > D$, $\mu_{1,\max} > D$). This leads to a low dilution rate ($D = 0.1$) due to the low value of $\max(m(A)) > D$ seen experimentally. We also choose a high substrate inflow $G_{\text{in}} \gg G_0$, so that the system is in glucose-excess conditions (assumption [A5.]).

For the selected functions and parameter values, the growth and inhibition curves are depicted in Figure 4. We graph them in terms of the original variables, glucose concentration, G (g/L), and acetate concentration , A (g/L), for ease of comparison to the experimental literature (Table 1). However, for the remainder of the analysis we will use the dimensionless variables and parameter values unless otherwise stated. We use the nondimensionalization in equations (8) and the parameter scalings:

$$\hat{\mu}_{1,\max} = \frac{\mu_{1,\max}}{D}\,,\ \hat{\mu}_{2,\max} = \frac{\mu_{2,\max}}{D}\,,\ \hat{K_G} = \frac{K_G}{G_{in}}\,, \tag{23}$$

$$\hat{K_A} = \frac{K_A}{r\,G_{in}}\,,\ \hat{K_{\text{IS}}} = \frac{K_{\text{IS}}}{r\,G_{in}}\,,\ \hat{K_{\text{IP}}} = \frac{K_{\text{IP}}}{r\,G_{in}}\,.$$

where $r = Y_{11}/Y_{21}$.

5.1. Monoculture and binary culture with no changes

In the monoculture system (10), for growth and inhibition functions (20)-(22) and parameter values in Table 2 and Table 3, we find a unique non-trivial equilibrium at

$$(x_1^m, G_1^m, A_1^m) = (2.72, 0.000418, 0.0197).$$

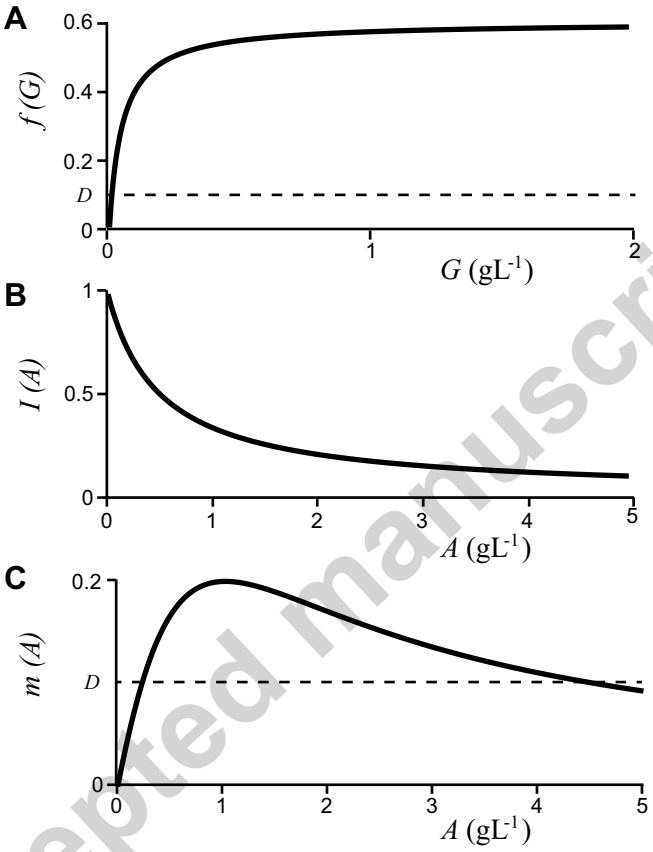

Figure 4: The functions $f(G)$, $I(A)$, and $m(A)$ (equations (20),(21), and (22), respectively), in the original (dimensional) variables, for the chosen parameter values.

In the binary culture system (9), there is one stable co-existence equilibrium point

$$(x^b_{1,S}, x^b_{2,S}, G^b_S, A^b_S) = (0.998, 1.70, 0.00159, 0.0337),$$

with $\bar{x}_S = 2.70$. There is also a stable equilibrium point where only x_1 survives at

$$(x^b_1, x^b_2, G^b, A^b) = (0.371, 0, 0.629, 0.371).$$

The biomass of the monoculture, $x = 2.72$, is greater than the total biomass in the binary culture at the stable co-existence equilibrium, $\bar{x} = x_1 + x_2 = 2.70$, as given by Theorem 3.

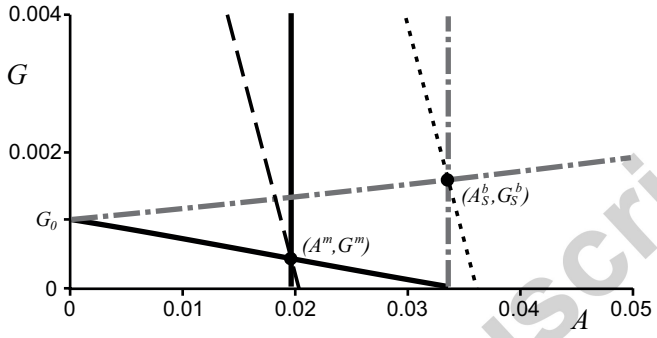

Figure 5: The curves G_1 and G_2, which determine the position of the monoculture equilibrium point(s) in the nondimensionalized system are shown in black solid lines, with the intersection labelled (A^m, G^m). The curves $f(G)I(A) = 1$ and $m(A) = 1$, which determine the position of the binary culture equilibrium point(s) are shown in grey dot-dash lines, with the intersection labelled (A^b_S, G^b_S). The lines of constant biomass for the monoculture and binary culture are black dashed and dotted lines, respectively.

5.2. Quantitative investigation of how to increase the binary culture's relative productivity

In chemostat experiments, a binary culture of this type shows a biomass increase of around 20% over the wild-type monoculture system [3]. In Figure 5 we plot the curves that determine the equilibrium points of the systems. The biomass is determined by the values of G and A, given in equations (15) and (16), thus in the (A, G)-plane, the curves $G = c - A/(1 + \gamma)$, for a constant $c = 1 - \gamma x_c/(\gamma + 1)$, are the lines of constant biomass, x_c. In order for the binary culture biomass to exceed that of the monoculture, the binary culture system must be modified such that the point (A^b, G^b) crosses the dashed line in Figure 5, or, alternatively, the monoculture system must be modified such that the point (A^m, G^m) crossed the dotted line in Figure 5. (The only exception to this is if Y_{11} or G_{in} are varied between the two systems, as these parameters appear in the non-dimensionalization of the biomass variables.)

5.2.1. Varying growth rates independently

When microbes specialize to grow on a single substrate they are found to increase their growth rate. One explanation for this is that they are able to allocate more resources to synthesizing transporters that increase the substrate uptake rate. By making the substitutions in equation (18), we can use parameters, α_1 and α_2 to modify the growth rates independently and perform a more general investigation.

To increase the growth rate of the microbes in the binary culture compared to monoculture we set $\alpha_1 > 1$, or $\alpha_2 > 1$, or both. It is important to note that increasing α_i will increase the growth rate of the pathway i by the factor α_i across all substrate concentrations.

- If we only increase the maximal growth rate of the glucose metabolism, α_1, we cannot increase the total biomass of the binary culture to match that of the monoculture, even if $\alpha_1 \to \infty$.
- If we only increase the maximal growth rate of the acetate metabolism, α_2, the binary culture has the same biomass of the monoculture at $\alpha_2 = 1.69$, i.e, the growth rate has to increase 69%.
- Finally, we allow both α_1 and α_2 to increase then we find multiple combinations of α_1, α_2 where the biomass has the same or larger mass than the monoculture. The combination of multipliers with minimal value of the sum $\alpha_1+\alpha_2$ for which the total biomass of the binary culture matches that of monoculture is when we only increase the second pathway, so $\alpha_1 = 1$ and $\alpha_2 = 1.69$.

Increases of around 15-20% have been seen experimentally when microbes have been grown on a single substrate. The increases of 70% that are required here are not realistic. Moreover, Bernstein et al. [3] observed biomass increase of 20% in chemostat experiments. Even increasing $\alpha_2 \to \infty$ the binary culture biomass never reaches 20% more than the monoculture

5.2.2. Increasing the substrate affinity in the binary culture

In *E. coli* the experimentally observed glucose affinity varies by orders of magnitude in different experimental conditions ($K_m = 0.0053 - 99$g/L [59]). This is because the bacteria have many different systems to transport and metabolize glucose as a substrate, that all have differing speeds and affinities. If we predict that the glucose specialist (x_1) in the binary system has an increasing substrate (glucose) affinity, we can investigate the effect this would have on biomass production by decreasing K_G in our model.

- Varying K_G we find that there there is no decrease in K_G that will lead to the binary system having a higher biomass than the monoculture system. This is expected from our results in Section 5.2.1, since $f(G) \approx \mu_{1,\max} G/K_G$ at low G, and there is no α_1 that leads to the binary system biomass exceeding that of the monoculture.

Additionally, the phenomenon whereby *E. coli* in low glucose conditions use higher affinity transporters would be predicted to occur in both the monoculture and primary microbe in the binary culture, as this depends mostly on growth conditions. If glucose affinities increase but remain equal, the monoculture will still outperform the binary culture by Theorem 3.

If the acetate scavenger specialist (x_2) in the binary culture has an increased acetate substrate affinity, relative to the monoculture, we can investigate the effect this would have on biomass production by decreasing K_A and K_{IS} in our model.

- Varying K_A (and K_{IS}) we find that the binary culture has higher biomass when K_A and K_{IS} decreases to 54% of the monoculture values i.e. an increase in substrate affinity of 85%. This is to be expected from our results in Section 5.2.1, as increasing $m(A)$ by 69% gave a higher biomass for the binary culture, and thus decreasing K_A (which increases the growth rate at low A values) should have a similar effect.

Note: we decrease K_{IS} concurrently with K_A in order to keep $\max(m(A))$ constant, however, if we only decrease K_A and allow $\max(m(A))$ to increase we see similar results (55% decrease cf. 54% decrease).

A two fold increase in the acetate affinity (halving the K_m value) is within realistic realms, and brings the K_m value of acetate metabolism to 0.12g/L. However, the higher-affinity *acs* pathway, that would be required for an increased acetate affinity, is more energy intensive (lower yield); this means that although the increased substrate affinity would act to increase the biomass, the consequent decrease in yield would counteract this increase. In our model formulation, we cannot directly account for the use of different acetate assimilation pathways between the binary culture system and the monoculture in the comparison, as we do not include the two pathways separately. Furthermore, up-regulation of the higher affinity *acs* pathway has been observed *in vivo* in wild-type *E. coli* [68] growing on acetate as well, so we consider it difficult to justify an change that increases the binary culture acetate affinity by 85% more than that of the monoculture.

If we take our analysis one step further and attempt to match the observed biomass increase of 20% in the binary culture [3], we find that there is no increase in substrate affinity ($K_m \to 0$) which can produce the required increase in biomass.

5.2.3. Varying form of the monoculture growth rate

When there is glucose available, *E. coli* will preferentially consume glucose due to catabolite repression until the acetate concentration gets too high, at which point the *E. coli* will switch to consuming acetate [41, 68]. This effect is incorporated implicitly into our model, as for high G, low A, $f(G)I(A) > m(A)$ and $\mu_{WT} \approx \mu_1$. Whereas, for high A we find $m(A) > f(G)I(A)$, and $\mu_{WT} \to \mu_2$. However, there may be some additional trade-off in the ability of the cell to produce the enzymes required for each pathway, so the increased utilization of

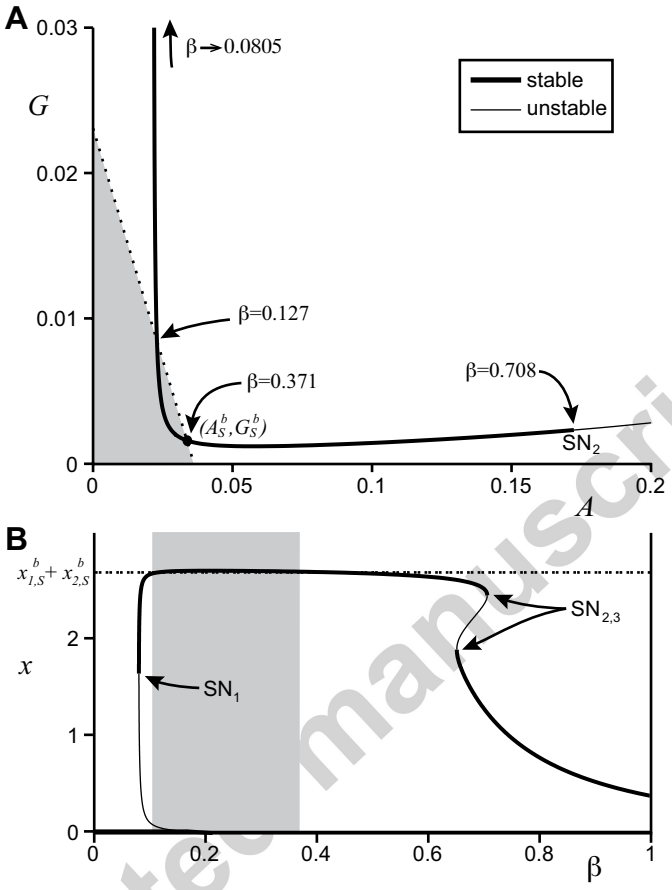

Figure 6: Panel (a) shows the position of the monoculture equilibrium point in the (A, G)-plane as β varies as a solid black line. The coexistence equilibrium point of the binary culture (A_S^b, G_S^b) is shown as a filled black circle. The dotted line shows the line of constant biomass for the binary culture at the coexistence equilibrium point, equilibrium points to the left of the curve (the shaded area) have a higher biomass than the binary culture. Important β values are labelled on the figure. Saddle-node bifurcations are labelled $SN_{1,2,3}$, but only SN_2 is within the range of this figure. Panel (b) shows the biomass (x value) of the monoculture equilibrium point as β varies is shown as a solid black line; thick where it is stable, thin where it is unstable. The dashed line shows the biomass of the comparative binary culture system, $x_{1,S}^b + x_{2,S}^b$, and the shaded region represents the β values where the monoculture has higher biomass than the binary culture system.

one pathway may decrease the growth rate of the other [42]. We can incorporate this into the model by using the modified growth function for the monoculture system in equation (19).

In experiments it is observed that the utilization of the two pathways, and thus the value of the parameter β, depends on the concentration of acetate A [68]. We will not assume a form for the dependence of β on A, however, by considering the existing experimental evidence we can determine whether the equilibrium acetate concentration and pathway utilization for a given β value is a realistic scenario.

The position in the (A, G)-plane of the equilibrium point for the modified monoculture system as β varies is shown in Figure 6(a). For β values $(0.127 < \beta < 0.371)$ the monoculture equilibrium point is to the left of the dotted line (binary culture biomass equivalence), and thus has a higher biomass. As β decreases below $\beta = 0.127$ the monoculture equilibrium G value increases, until the monoculture does metabolize enough glucose to survive and the equilibrium point disappears in a saddle-node bifurcation at $\beta = 0.0805$ (SN_1). As β increases from $\beta = 0.371$, the monoculture equilibrium point disappears in a saddle-node bifurcation at $\beta = 0.708$ (SN_2). The system becomes bi-stable at $\beta = 0.653$ (SN_3), shown in Figure 6(b). The lower biomass equilibrium point persists and reaches the x_1-only equilibrium point of the binary culture (A_1, G_1) at $\beta = 1$.

At $\beta = 1$ the monoculture is the equivalent of the binary culture system with $x_2 = 0$, which means it has a lower biomass than the binary culture system coexistence equilibrium point (not shown in Figure 6). As β decreases from 1, the advantage of being able to consume the acetate increases the monoculture's biomass. We find that the binary culture only has higher biomass than the monoculture for $\beta > 0.371$. However, for $\beta > 0.371$ the monoculture reaches an equilibrium point with high acetate concentration, but *E. coli* are observed to switch to consuming more acetate when the acetate concentration increases [68], which means that these high β values (a higher utilization of the glucose consumption pathway $f(G)I(A)$ over the acetate consumption pathway $m(A)$) are unrealistic.

As $\beta \to 0$, the monoculture growth rate is increasingly dependent on the second pathway, $m(A)$, which consumes exclusively acetate A. Since glucose G is the only substrate provided to the chemostat, we expect that the monoculture will not survive. Indeed, for $\beta < 0.0805$ the monoculture washes out and the biomass of monoculture $(x = 0)$ will be less than the biomass of the binary culture.

The optimal β value (to maximize growth rate [1, 13, 35]) will depend on the concentration of G and A. However, for monoculture equilibrium values as β varies the growth rate is set to D by the chemostat dynamics. If we instead predict that the optimal β value would lead to a higher biomass, we find peak monoculture biomass at $\beta = 0.208$ ($x^m = 2.71$), and we reach the conclusion that the monoculture would be expected to have a higher biomass than the binary culture.

5.2.4. Varying yields

In this section we examine the effect of varying yields in our model of *E. coli* growing on glucose. If the microbes in the binary culture are able to reduce their energy requirements when they specialise to a single substrate, the yields Y_{11} and Y_{22} would increase. If we include the effect of the cost of transporting acetate into the cell, this would decrease Y_{22}. Here we will assume that the metabolic pathway stoichiometry is fixed, i.e., the ratio $r = Y_{11}/Y_{21}$ (grams of acetate produced per gram of glucose consumed) is fixed. The effects of varying the yields are as follows:

- By increasing Y_{11} (and Y_{21} as r is fixed) in the binary culture system, that is, reducing the amount of glucose G the primary consumer microbe requires to make one g of biomass x_1, the total biomass of the binary culture can exceed the monoculture biomass. In this example we find that the two systems have equal biomass when $\bar{Y}_{11} = 1.03\,Y_{11}$ (and $\bar{Y}_{21} = 1.03\,Y_{21}$), which represents an increase in glucose pathway efficiency of 3%.
- By increasing Y_{22} in the binary culture system, which corresponds to a reduction in the amount of acetate A the secondary scavenger microbe requires to make one gram of biomass x_2, the total biomass of the binary culture can exceed the monoculture biomass. In this example we find that the two systems have equal biomass with $\bar{Y}_{22} = 1.02\,Y_{22}$. This represents an increase in acetate pathway efficiency of 2%.

If the ratio $r = Y_{21}/Y_{11}$ is not fixed, we find that increasing Y_{11} independently of Y_{21}, we can get the same total biomass with $\bar{Y}_{11} = 1.01\,Y_{11}$, and decreasing Y_{21} independently of Y_{11} we find that $\bar{Y}_{21} = 0.98\,Y_{21}$ gives the same total biomass in both systems. However, in order for Y_{21} to decrease without Y_{11} decreasing (or Y_{11} to increase without Y_{21} increasing), the glucose consuming microbe would have to utilize different metabolic pathways, with different stoichiometry, that produce more A per G consumed. In experiments, it is observed that wild-type *E. coli* can modify their metabolic strategies depending on the environmental conditions, specifically, in excess acetate the monoculture is seen to increase the flux through the acetate-metabolism pathway $m(A)$ [68]. This would be equivalent to varying β in our modified monoculture system (equation (19)); the stoichiometry of the pathways would not change. In this application, we argue that it is unrealistic to modify Y_{21} independently of Y_{11}.

Finally, we can generate the 20% increase in biomass observed in Bernstein et al. [3] if we increase by the efficiency of the glucose-metabolism pathway (Y_{11} and Y_{21}) by 57%, or increase the efficiency of acetate-metabolism pathway, Y_{22}, by 34%.

6. Discussion

In this paper we describe a minimal model of a syntrophic chain system in which the metabolism of a substrate is divided into two distinct organisms. We compare this to a monoculture, which is able to completely metabolize the

substrate. Under very general assumptions we show that the monoculture will always produce larger biomass than the equivalent binary syntrophic chain system. This finding does not agree with experimental findings from microbial consortial systems, which show higher biomass for consortial systems [3]. Two key assumptions in the creation of our minimal model are that there are no metabolic advantages to dividing the metabolic steps into separate organisms, and that there is no cost to the monoculture for using multiple substrates concurrently. Since the model under these assumptions does not reproduce the increased biomass in the consortium that is observed experimentally, this leads us to conclude that one (or both) of these assumptions are incorrect and allows us to investigate the effect of making these assumptions more realistic. By modifying the minimal model we are able to test hypotheses and investigate the effects of adaptations that can develop in a syntrophic chain system, clarifying the mechanisms that contribute to the experimentally observed advantage. We find that that the division of metabolic pathways must have an effect on both the growth and yield of the system.

If we assume that in the binary culture the pathways are able to metabolize the substrate faster (increasing the growth rate), we find that it is sometimes possible to have a higher biomass in the binary culture system. However, considering a specific example from *E. coli* using typical parameters, the growth rate increases required are much larger than those observed experimentally when an organism adapts to a single food source. Considering instead the possibility of increases in substrate affinity, we find that, for the specific example of *E. coli*, a two-fold decrease in the acetate K_m value for the binary culture relative to the monoculture would lead to higher biomass. However, in similar low substrate conditions acetate affinity increases would be seen in both the monoculture and binary culture, and even if the acetate specialist in the binary culture could increase its substrate affinity, this wouldn't necessarily increase the productivity, as the higher affinity acetate assimilation pathway has a lower yield.

We also test a hypothesis that the efficiencies of the metabolic pathways in the binary culture are increased, as the specialists do not have to produce the enzymes related to the other pathways, reducing the amount of energy required for enzyme synthesis and maintenance, and thereby increasing the proportion of energy that can go towards biomass production [42]. By varying the yield, it is possible to increases the binary culture's biomass to match that of the monoculture with an increase of only 2-3% in the parameters Y_{11} or Y_{22}. This magnitude of yield change is within the range of what is observed experimentally, and we consider this to be the most likely cause of the observed productivity increase in the binary culture.

Comparing our results to past work on the question of whether organisms maximize growth rates or efficiency, we find that two main theories are the Maximum Power Principle (MPP) [9, 36, 56] and the Resource Ratio Theory (RRT) [38, 39, 62, 63]. The MPP states that systems strive to increase 'power' within the system constraints. This has been used to successfully predict the outcome of two species competition experiments [9]. The RRT states that the system/species that can use as much as possible of the resources available (have

the lowest amount of 'wasted' substrate) will win in a competition experiment (or will evolve). [38]. In summary, MPP argues for maximising substrate uptake rate, whereas RRT argues for optimizing the growth at low substrate concentrations. In a chemostat with fixed yield, the highest substrate uptake will correspond to the highest growth rate, and these two will be consistent. Thus, in evolution (or competition) in a chemostat, maximizing growth rate or maximizing substrate uptake rate may be advantageous strategies in order to survive.

In this work we are motivated by the observation of increased biomass in a division of labor system [3], which has important implications for industrial settings. We find that yield maximization should be the advantageous strategy for increasing the biomass production of a chemostat system. In all our work we consider the binary and monoculture systems in isolation, and investigate and compare the optimal productivity (biomass production) of these systems. We are not considering the evolution of these division of labor systems, as there is much work already investigating this and it is not the focus of our work. We are also not considering competition of these two systems, thus the arguments from RRT and MPP are not directly applicable to this situation. Some work has found that evolutionary advantage depends on the stress conditions, with some papers even finding that the 'optimal' robust state has lower biomass [45]. This is not unexpected as up-regulating pathways with higher substrate affinities is often more costly (decreased yield), but this enables survival at lower substrate concentrations and thus resistance to invasion.

For *E. coli* communities, the cross-feeding syntrophic chain system studied in section 5 has been seen to evolve repeatedly [50, 51, 64]. This suggests that there must be some increase in growth rate or substrate affinity following specialization in order for the system to out-compete the original monoculture. When synthetically engineered, this cross-feeding system has been found to have higher productivity [3]. Our model shows that increases in in growth rate or substrate affinity are not sufficient to explain this observed increase in productivity, and that an increase the efficiency (yield) of the syntrophic system must have occured.

An interesting contradiction that remains is that in the unmodified model $A_S^b > A^m$ for all parameters and growth functions, but in experiments the concentration of the inhibitory intermediate A is observed to be lower in a syntrophic chain system than in a monoculture. If we assume that an increase in efficiency when organisms specialize to a single substrate is sufficient to explain the observed increase in biomass, we find that there is no decrease in A_S^b in the binary culture when we increase the yield Y_{22} and only a small decrease when we increase the yield Y_{11}. However, increasing the growth rates in the binary system does decrease A_S^b. This suggests that increases in both yield (increased efficiency) and growth kinetics play a role in metabolic specialisation. By applying our model to experimental data, we will be able to investigate these factors in future work.

A. Binary culture equilibrium points existence and stability

In this appendix we prove Theorem 1.

A.1. Existence of equilibrium points

Equilibrium points in the binary system (9) must satisfy

$$(f(G)I(A) - 1)x_1 = 0, \tag{24}$$
$$(m(A) - 1)x_2 = 0, \tag{25}$$
$$1 - G - f(G)I(A)x_1 = 0, \tag{26}$$
$$-A + f(G)I(A)x_1 - \gamma\, m(A)x_2 = 0, \tag{27}$$

a. A trivial equilbrium point, where $x_1 = 0$, $x_2 = 0$, must satisfy $1 - G = 0$ from equation (26) and $-A = 0$ from equation (27). This exists for all functions and parameter values at $(x_1, x_2, G, A) = (0, 0, 1, 0)$.

b. A boundary equilibrium point where only x_1 survives ($x_1 \neq 0$) must satisfy:

$$\begin{aligned} f(G)I(A) - 1 = 0 \quad &\text{from equation (24),} \\ 1 - G - f(G)I(A)x_1 = 0 \quad &\text{from equation (26),} \\ -A + f(G)I(A)x_1 = 0 \quad &\text{from equation (27).} \end{aligned}$$

A single boundary equilibrium point exists at

$$(x_1^1, x_2^1, G^1, A^1) = (1 - G^1, 0, G^1, 1 - G^1),$$

where G^1 is the solution to $f(G^1)I(1 - G^1) = 1$.

c. Co-existence equilibrium points, where both x_1 and x_2 survive, are positive solutions $(x_1, x_2, G, A) \in \mathbb{R}^4_+$ that satisfy

$$f(G)I(A) - 1 = 0 \quad \text{from equation (24),} \tag{28}$$
$$m(A) - 1 = 0 \quad \text{from equation (25),} \tag{29}$$

and equations (26) and (27). The co-existence equilibria take the form $(1 - G_i^b, (1 - G_i^b - A_i^b)/\gamma, G_i^b, A_i^b)$ for $i = S, U$, where A_i^b are the solutions of $m(A) = 1$ (see Figure 1(a.)), and G_i^b are the solutions to $f(G)I(A_i^b) = 1$ (see Figures 1(b.) and 1(c.)).

Given Assumption [A5.] in Section 2.3, equation (29) has two positive solutions A_S^b and A_U^b, where $A_S^b < A_U^b$ (Figure 1(a)).

For each of these A^b values, equation (28) has a unique positive solution for G^b, if and only if $1/I(A^b) < \mu_{1,\max}$ (as shown in Figures 1(b.) and(c.)). Thus, we define the critical A value by $I(A^b_{\text{crit}}) = 1/\mu_{1,\max}$. For $A^b < A^b_{\text{crit}}$ there is a unique positive G^b.

From equations (26) and (27) the biomass at equilibrium is given by $x_1^b = 1 - G^b$ and $x_2^b = (1 - G^b - A^b)/\gamma$. Thus, the biomass of x_2 is only positive if $1 - G^b - A^b > 0$.

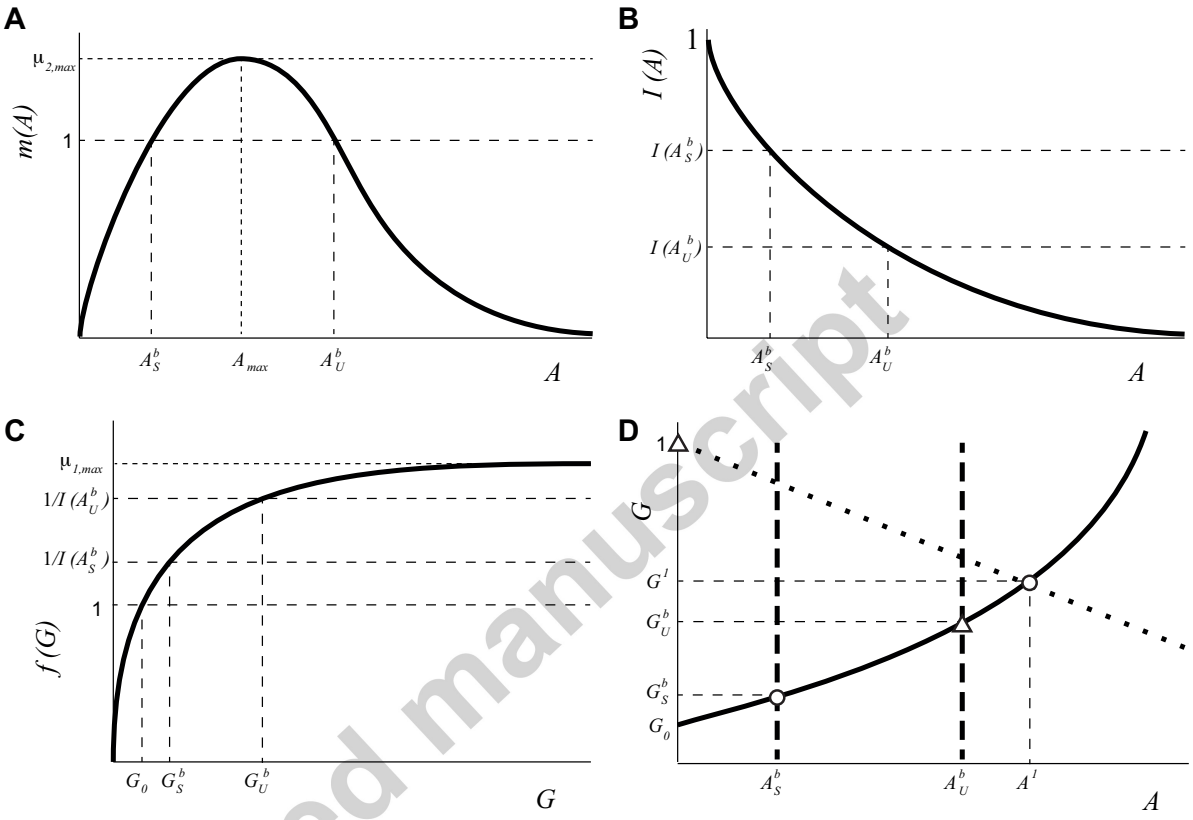

Figure 1: Qualitative sketches of the growth and inhibition curves and positions of equilibria for the case where there are two co-existence equilibrium points. Panel (a.) shows the function $m(A)$ showing A_{max} and the relative positions of A_S^b and A_U^b. Panel (b.) shows the function $I(A)$ with the relative positions of A_S^b and A_U^b. Panel (c.) shows function $f(G)$ and the relative positions of G_S^b and G_U^b. The position of G_0 defined by $f(G) = 1$ is shown as well. Panel (d.) shows the curves $f(G)I(A) = 1$ (solid black curve) and $m(A) = 1$ (dashed black lines). The co-existence equilibrium points projected to (A, G) plane are at the two intersections of these curves. The dotted black line $G = 1 - A$ (together with the solid black curve $f(G)I(A) = 1$) determines the position of the boundary ($x_2 = 0$) equilibrium point projected into the (A, G) plane. The position of G_0 defined by $f(G) = 1$ is shown as well.

The co-existence equilibrium points are the intersections of the curves implicitely defined by $f(G)I(A) = 1$ and $m(A) = 1$. The equation $m(A) = 1$ defines two vertical lines $A = A^b_S$ and $A = A^b_U$ in the (A, G) plane. The slope of the curve $h := \{(A, G) \in \mathbb{R}^2_+ \mid f(G)I(A) = 1\}$ is given by:

$$\frac{dh}{dA} = \frac{-f\frac{\partial I}{\partial A}}{\frac{\partial f}{\partial G}I} \tag{30}$$

From assumptions [A2.] and [A3.] this gives $\frac{dh}{dA} > 0$ for all (A, G). The curve has a vertical asymptote at A^b_{crit}. As $A \to A^b_{crit}$, we find that $f(G) \to \mu_{1,\max}$, $I(A) \to 1/\mu_{1,\max}$, $G \to \infty$, $\frac{\partial f}{\partial G} \to 0$, and $\frac{\partial I}{\partial A} < 0$. Combining this information, the numerator of $\frac{dh}{dA}$ is positive and bounded away from zero, while the denominator of $\frac{dh}{dA}$ goes to zero, thus $\frac{dh}{dA} \to \infty$ as $A \to A^b_{crit}$ from below. The assumptions [A1.]-[A6.] give six possible cases for the intersections of these curves (shown in Figure 2). Their intersection is the projection of the co-existence equilibrium points to (A, G) plane.

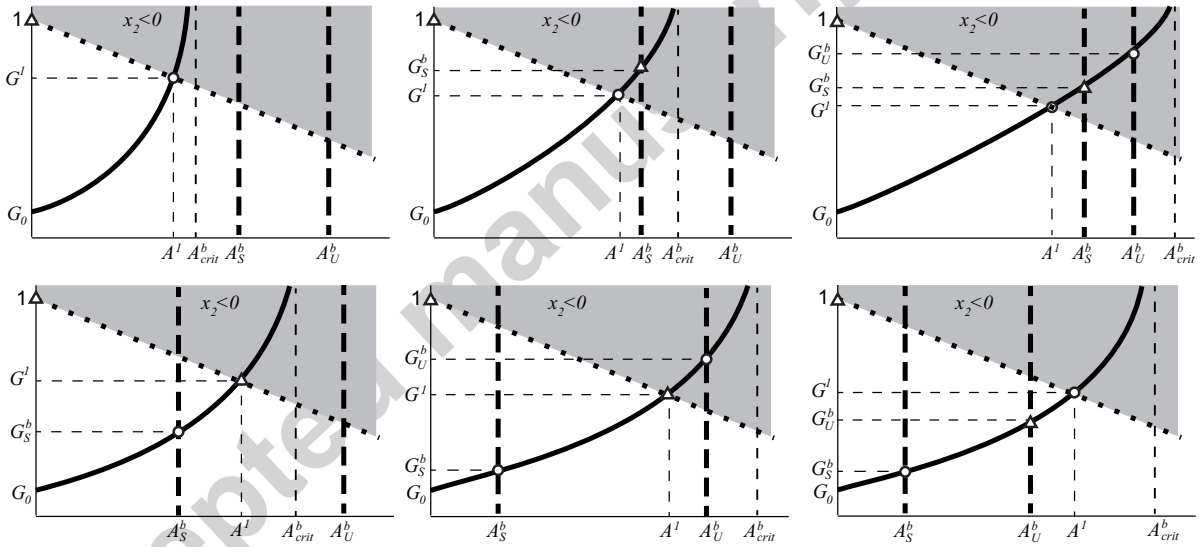

Figure 2: Qualitative sketches of the six possible cases based on assumptions [A1.]-[A4.] in Section 2.3. Equilibrium points are marked with a circle for stable equilibria and a triangle for unstable equilibria. In the shaded grey region ($G > 1 - A$) any solutions are physically unrealistic as $x_2 < 0$. The trivial ($x_1 = 0$, $x_2 = 0$) equilibrium point at (0,1) is shown. For all cases, there is a boundary ($x_2 = 0$) equilibrium point (A^1, G^1) which, when projected into the (A, G) plane, lies at the intersection of the dotted black line $G = 1 - A$ together with the solid black curve $f(G)I(A) = 1$. The curves $f(G)I(A) = 1$ (solid black curve) and $m(A) = 1$ (dashed black lines) are shown, the position of co-existence equilibrium points projected to (A, G) plane are at the intersections of these curves. The vertical asymptote of the curve $f(G)I(A) = 1$ is labelled A^b_{crit}. The position of G_0 defined by $f(G) = 1$ is shown as well.

- There are no co-existence equilibria in the following three cases:

  (i) If $A^b_{\text{crit}} < A^b_S$, then $1/I(A^b_S) > \mu_{1,\max}$ and there are no solutions to equation (29) for $A = A^b_S$ or $A = A^b_U$. Thus, there are no co-existence equilibria.

  (ii) If $A^b_S < A^b_{\text{crit}} < A^b_U$ and $G^b_S + A^b_S > 1$. Then $1/I(A^b_S) < \mu_{1,\max}$ and equation (29) with $A = A^b_S$ has solution $G = G^b_S$, but $1/I(A^b_U) > \mu_{1,\max}$ and there are no solutions to equation (29) with $A = A^b_U$. However, as $1 - G^b_S - A^b_S < 0$, $x^b_{2,S} < 0$ and there are no (positive) co-existence equilibria.

  (iii) If $A^b_U < A^b_{\text{crit}}$ and $G^b_S + A^b_S > 1$. Then $1/I(A^b_S) < \mu_{1,\max}$ and equation (29) with $A = A^b_S$ has solution $G = G^b_S$, and $1/I(A^b_U) < \mu_{1,\max}$ equation (29) with $A = A^b_U$ has solution $G = G^b_U$. However, as $1 - G^b_S - A^b_S < 0$, $x^b_{2,S} < 0$ and since$G^b_U > G^b_S$ and $A^b_U > A^b_S$ $1 - G^b_U - A^b_U < 1 - G^b_S - A^b_S < 0$ so $x^b_{2,U} < 0$, and there are no (positive) co-existence equilibria.

- There is a single co-existence equilibrium point in the following two cases:

  (i) If $A^b_S < A^b_{\text{crit}} < A^b_U$, then $1/I(A^b_S) < \mu_{1,\max}$ and equation (29) with $A = A^b_S$ has solution $G = G^b_S$, but $1/I(A^b_U) > \mu_{1,\max}$ and there are no solutions to equation (29) with $A = A^b_U$. If $1 - G^b_S - A^b_S > 0$, then $x^b_{1,S} > 0$ and $x^b_{2,S} > 0$ and there is one co-existence equilibrium point $S := (x^b_{1,S}, x^b_{2,S}, G^b_S, A^b_S)$.

  (ii) If $A^b_U < A^b_{\text{crit}}$, then equation (29) with $A = A^b_S$ and $A = A^b_U$ has corresponding solutions $G = G^b_S$ and $G = G^b_U$, where $G^b_S < G^b_U$ (see Figure 1(d.)). If $1 - G^b_U - A^b_U < 0 < 1 - G^b_S - A^b_S$, then co-existence equilibrium point $S := (x^b_{1,S}, x^b_{2,S}, G^b_S, A^b_S)$ exists, but $x^b_{2,U} < 0$ so S is the only co-existence equilibrium point.

- There are two co-existence equilibria in the following case:

  (i) If $A^b_U < A^b_{\text{crit}}$, then equation (29) with $A = A^b_S$ and $A = A^b_U$ has corresponding solutions $G = G^b_S$ and $G = G^b_U$, where $G^b_S < G^b_U$ (see Figure 1(d.)). If $1 - G^b_U - A^b_U > 0$, then $1 - G^b_S - A^b_S > 0$ and $x^b_{1,S} > 0$, $x^b_{2,S} > 0$, $x^b_{1,U} > 0$, and $x^b_{2,U} > 0$. Therefore there are two co-existence equilibrium point $S := (x^b_{1,S}, x^b_{2,S}, G^b_S, A^b_S)$ and $U := (x^b_{1,U}, x^b_{2,U}, G^b_U, A^b_U)$.

A.2. Stability of equilibrium points

We introduce the following variables:

$$w_1(t) = G(t) + x_1(t), \tag{31}$$

$$w_2(t) = G(t) + \gamma x_2(t) + A(t). \tag{32}$$

Note that the system obeys a conservation law of material consumed to biomass produced. The rate equations for these new variables are:

$$\dot{w_1} = 1 - w_1 \tag{33}$$

$$\dot{w_2} = 1 - w_2. \tag{34}$$

which means that the set $\Omega^b := \{(x_1, x_2, G, A) \in \mathbb{R}^4_+ \ : \ x_1 = 1 - G,\ \gamma x_2 = 1 - G - A\}$ is an exponentially attracting two-dimensional invariant subspace of the full $\mathbb{R}^4$ phase space. The asymptotic behaviour of the system is determined by the dynamics on Ω^b, given by

$$\dot{G} = 1 - G - f(G)I(A)x_1(G), \tag{35}$$

$$\dot{A} = -A + f(G)I(A)x_1(G) - \gamma m(A)x_2(G, A), \tag{36}$$

with $x_1(G) = 1 - G$, $x_2(A, G) = (1 - G - A)/\gamma$. In this reduced system, we consider the region where $x_1 \geq 0, x_2 \geq 0$, given by $G \leq 1 - A$ in the positive quadrant. The Jacobian of this reduced system is:

$$J(G, A) = \begin{bmatrix} -1 + fI - \frac{\partial f}{\partial G} I x_1 & -f\frac{\partial I}{\partial A} x_1 \\ -fI + \frac{\partial f}{\partial G} I x_1 + m & -1 + f\frac{\partial I}{\partial A} x_1 - \gamma \frac{\partial m}{\partial A} x_2 + m \end{bmatrix}, \tag{37}$$

where $x_1 = 1 - G$, $x_2 = (1 - G - A)/\gamma$. The trivial equilibrium point $(x_1, x_2, G, A) = (0, 0, 1, 0)$, $I(0) = 1$ and $m(0) = 0$ (from Assumptions [A3.] and [A4.]) and the Jacobian becomes:

$$J(G, A) = \begin{bmatrix} -1 + f(1) & 0 \\ -f(1) & -1 \end{bmatrix}, \tag{38}$$

which has eigenvalues $\lambda =, -1, f(1) - 1$. From Assumption [A2.] in Section 2.3 we know that $0 < f(1) < \mu_{1,\max}$. When $f(1) > 1$ the trivial equilibrium will have three negative eigenvalues (two from the components normal to Ω^b and one from the 2D reduced subsystem) and one positive eigenvalue, thus it is an unstable saddle. The condition $f(1) > 1$, which corresponds to $f(G_{\text{in}}) > D$ in the original dimensions, is ensured by assumption [A6.]: the trivial equilibrium point will be unstable as long as the substrate inflow is in excess.

The boundary equilibrium point ($fI = 1$,$x_2 = 0$) has the Jacobian

$$J(G^1, A^1) = \begin{bmatrix} -\frac{\partial f}{\partial G} I x_1 & -f\frac{\partial I}{\partial A} x_1 \\ -1 + \frac{\partial f}{\partial G} I x_1 + m & -1 + f\frac{\partial I}{\partial A} x_1 + m \end{bmatrix}. \tag{39}$$

From this we find $\text{Tr}(J) = -\left[\left(\frac{\partial f}{\partial G} I - f\frac{\partial I}{\partial A}\right) x_1 + (1 - m)\right]$ and $\text{Det}(J) = (1 - m)\left[\frac{\partial f}{\partial G} I - f\frac{\partial I}{\partial A}\right] x_1(G)$. The boundary equilibrium point undergoes transcritical bifurcations when $m(A) = 1$, i.e., when $A^1 = A^b_S$ and $A^1 = A^b_U$. For $A^1 < A^b_S$, $m(A^1) < 1$, $\text{Det}(J) > 0$, $\text{Tr}(J) < 0$, and $(Tr^2 - 4 \cdot Det) > 0$ and the equilibrium point is a stable node. For $A^b_S < A^1 < A^b_U$, $m(A^1) > 1$, $\text{Det}(J) < 0$ and the equilibrium point is an unstable saddle. For $A^b_U < A^1$, $m(A^1) < 1$, $\text{Det}(J) > 0$, $\text{Tr}(J) < 0$, and $(Tr^2 - 4 \cdot Det) > 0$ and the equilibrium point is a stable node again. The vector $(A, G) = (1, -1)$ is a stable eigenvector which lies on the $x_2 = 0$ invariant line: $G = 1 - A$.

For the co-existence equilibria ($fI = 1$,$m = 1$) the Jacobian becomes:

$$J(G, A) = \begin{bmatrix} -\frac{\partial f}{\partial G} I x_1 & -f\frac{\partial I}{\partial A} x_1 \\ \frac{\partial f}{\partial G} I x_1 & f\frac{\partial I}{\partial A} x_1 - \gamma \frac{\partial m}{\partial A} x_2 \end{bmatrix}, \tag{40}$$

with $\mathrm{Tr}(J) = -\left[\left(\frac{\partial f}{\partial G}I - f\frac{\partial I}{\partial A}\right)x_1(G) + \gamma\frac{\partial m}{\partial A}x_2(G,A)\right]$ and $\mathrm{Det}(J) = \frac{\partial f}{\partial G}Ix_1(G)\gamma\frac{\partial m}{\partial A}x_2(G,A)$.

For (A_S^b, G_S^b) in the region $x_2 > 0$, $\mathrm{Tr}(J) < 0$ and $\mathrm{Det}(J) > 0$, and $(Tr^2 - 4 \cdot Det) > 0$ so the equilibrium point is a stable node. For (A_U^b, G_U^b) in the region $x_2 > 0$, $\mathrm{Det}(J) < 0$ and the equilibrium point is an unstable saddle. These equilibrium points go through transcritical bifurcations at $x_2 = 0$ when they pass through the boundary equilibrium point. Details are shown in Figure 2.

B. Monoculture equilibrium points

In this appendix we prove Theorem 2.

B.1. Existence

Given assumptions [A1.]-[A6.]

a. The monoculture system (10) has a trivial equilibrium point with $x = 0$, which must satisfy $1 - G = 0$ and $-A = 0$. This equilibrium point lies at $(x, G, A) = (0, 1, 0)$ for all functions and parameters.

b. Any non-trivial, $x \neq 0$, equilibrium points must satisfy

$$f(G)I(A) + m(A) - 1 = 0\,, \tag{41}$$

$$1 - G - f(G)I(A)x = 0\,, \tag{42}$$

$$-A + (f(G)I(A) - \gamma m(A))x = 0\,, \tag{43}$$

Eliminating $f(G)$, $I(A)$, and $m(A)$ from equations (41)-(43) yields the equation for equilibrium biomass

$$x = \left(1 + \frac{1}{\gamma}\right)(1 - G^m) - \frac{A^m}{\gamma}\,, \tag{44}$$

where G^m and A^m lie in the intersection of the curves

$$G_1 := \{(x, G, A) \in \mathbb{R}^3_+ : f(G)I(A) + m(A) = 1\}, \tag{45}$$

and

$$G_2 := \{(x, G, A) \in \mathbb{R}^3_+ : G = 1 - \frac{A}{1 + \gamma - \frac{\gamma}{1 - m(A)}}\}. \tag{46}$$

To determine the number of non-trivial equilibrium points, we must consider the shape and position of the curves G_1 and G_2 to find intersection points.

B.1.1. Shape and position of G_1

The curve G_1 has the following properties:

- The intersection of the curve G_1 with G axis ($A = 0$) satisfies $f(G) = 1$. Note that this equation has a unique solution since f is monotonically increasing and has $\mu_{1,max} > 1$. We label this intersection G_0.

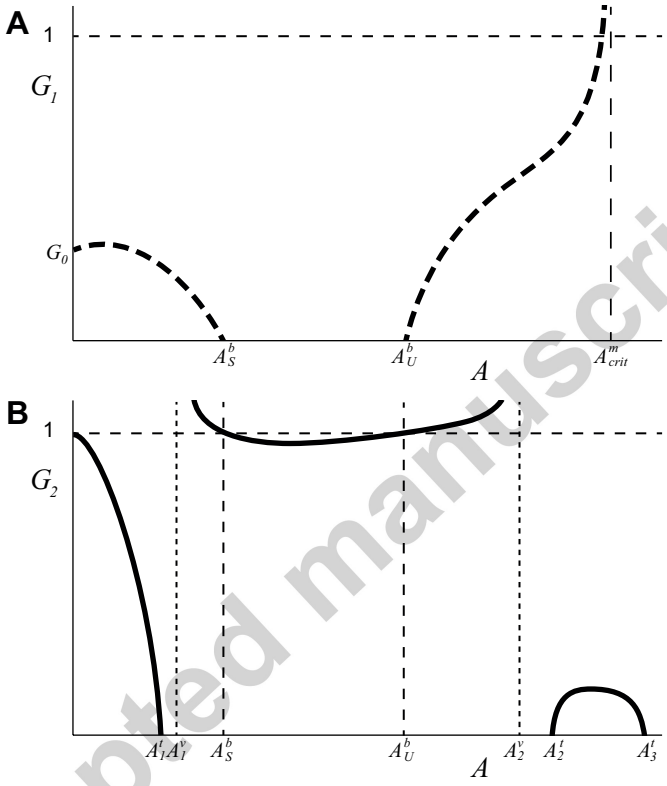

Figure 1: (a) Qualitative sketch of the curve G_1 implicitly defined by (45). (b) Qualitative sketch of the curve G_2 defined by (46).

- The intersection of the curve G_1 with A axis ($G = 0$) satisfies $m(A) = 1$, which has two solutions, A_S^b and A_U^b. We note for future reference that these values correspond to the equilibrium acetate concentration solutions for the binary system.

- Since $D_G(f(G)I(A) + m(A) - 1) \neq 0$ for all $G > 0$, $A > 0$ by the implicit function theorem, there is a scalar function h such that

$$f(h(A))I(A) + m(A) = 1$$

and thus the points on G_1 satisfy $G = h(A)$.

- Implicitly differentiating equation (45) we get an expression for the slope of this curve in (G, A) space:

$$\frac{\partial}{\partial A}\left(f(h(A))I(A) + m(A) - 1\right) = 0$$
$$\frac{\partial(fI)}{\partial h} \cdot \frac{dh}{dA} + \frac{\partial(fI)}{\partial A} + \frac{\partial m}{\partial A} = 0,$$

which we can rearrange to give the expression for the derivative of the function $G = h(A)$

$$\frac{dh}{dA} = \frac{-\left(\frac{\partial(fI)}{\partial A} + \frac{\partial m}{\partial A}\right)}{\frac{\partial(fI)}{\partial G}}. \tag{47}$$

We now try to determine the sign of this derivative from Assumptions [A2.]-[A4.] in Section 2.3. First we note that

$$\frac{\partial(fI)}{\partial G} > 0 \quad \text{for all } (G, A), \qquad \frac{\partial(fI)}{\partial A} < 0 \quad \text{for all } (G, A),$$

$$\frac{\partial m}{\partial A} > 0 \quad \text{for } A < A_{max}, \qquad \frac{\partial m}{\partial A} < 0 \quad \text{for } A > A_{max}.$$

The discussion that follows is illustrated in Figure 1 (a).

- For the lower branch of the curve ($A < A_{max}$), $\frac{\partial(fI)}{\partial A} < 0$ but $\frac{\partial m}{\partial A} > 0$, so the sign of $\frac{dh}{dA}$ is not determined by our assumptions. However, since the lower branch intersects G axis in a point $(0, G_0)$ and the A-axis at $(A_S^b, 0)$, the derivative $\frac{dh}{dA}$ must become negative for some interval (A, A_S^b).

- For the upper branch of the curve ($A > A_{max}$) we know that $\frac{dh}{dA} > 0$ and that the curve intersects the A-axis at $A = A_U^b$. As A increases, $f(G)I(A) \to 0$ and $m(A) \to 0$. At a critical A value, implicitely defined by $\mu_{1,\max} I(A) + m(A) = 1$, the curve reaches a vertical asymptote, A_{crit}^m, and for $A_{crit}^m < A$ there is no solution to $f(G)I(A) + m(A) = 1$.

B.1.2. Shape and position of G_2

We rewrite equation (46) as $G_2 = 1 - H(A)$, where

$$H(A) = \frac{A}{1+\gamma-\frac{\gamma}{1-m(A)}}\,.$$

We summarize our observations about curve $G_2 = G_2(A)$.

- When $A = 0$, $H(A) = 0$ and so the curve G_2 intersects the G-axis at $G = 1$.
- The intersection of the curve $G_2 = 1 - H(A)$ with A-axis satisfies $H(A) = 1$. This solution, which we denote A^t satisfies $1 + \gamma - \frac{\gamma}{1-m(A^t)} = A^t$, or rewritten, $m(A^t) = 1 - \frac{\gamma}{1+\gamma-A^t}$. This equation always has one solution, in the region $0 < A^t < A_S^b$, and in some cases can have two more solutions for high $A_U^b < A^t < 1$, as shown in Figure Figure 3. The intersections with the A-axis will be ordered by increasing A with subscripts A_1^t and A_2^t, A_3^t (if applicable).
- The curve $G_2 = 1-H(A)$ has vertical asymptotes when $1+\gamma-\frac{\gamma}{1-m(A)} = 0$, which correspond to the value A satisfying $1 + \gamma = \frac{\gamma}{1-m(A)}$. There is one asymptote in the region $A < A_S^b$ ($m(A) < 1$), which follows from the fact that the left hand side is bounded and the right hand side grows without bound as $A \to A_S^b$, since $m(A_S^b) = 1$ by definition. In the region $A > A_U^b$ ($m(A) < 1$), there is one asymptote, as the left hand side is bounded and the right hand side grows without bound as $A \to A_U^b$ from above, since $m(A_U^b) = 1$ by definition. We denote the asymptotic values of A by A_1^v and A_2^v, which satisfy $m(A_i^v) = \frac{1}{1+\gamma}$, shown in Figure 3.
- For A_1^v and A_1^t, which are both in the region $A < A_S^b$ we wish to determine their relative positions. Consider equations $1 + \gamma = \frac{\gamma}{1-m(A^v)}$ and $1 + \gamma = A^t + \frac{\gamma}{1-m(A^t)}$. It follows that

  $$A^t + \frac{\gamma}{1-m(A^t)} = \frac{\gamma}{1-m(A^v)}\,.$$

  and since $0 < A^t < 1$ this means that

  $$\frac{\gamma}{1-m(A^t)} < \frac{\gamma}{1-m(A^v)}\,,$$

  In the region $A < A_S^b$ the function $\frac{\gamma}{1-m(A)}$ is increasing as A increases, thus $A_1^t < A_1^v$. In the region $A > A_U^b$ the function $\frac{\gamma}{1-m(A)}$ is now decreasing as A increases, thus (if A_2^t and A_3^t exist) $A_2^v < A_2^t < A_3^t$.

- The slope of the curve is given by:

$$\begin{aligned}\frac{dG_2}{dA} &= -\frac{dH(A)}{dA} \\ &= -1 \cdot \frac{\left(1+\gamma-\frac{\gamma}{1-m(A)}\right) - A\frac{d}{dA}\left(\frac{-\gamma}{1-m(A)}\right)}{\left(1+\gamma-\frac{\gamma}{1-m(A)}\right)^2} \\ &= -1 \cdot \frac{\left(1+\gamma-\frac{\gamma}{1-m(A)}\right) + \frac{dm(A)}{dA}\frac{\gamma A}{(1-m(A))^2}}{\left(1+\gamma-\frac{\gamma}{1-m(A)}\right)^2} \end{aligned} \tag{48}$$

- For $0 < A < A_1^v$, $1+\gamma-\frac{\gamma}{1-m(A)} > 0$ and $\frac{dm(A)}{dA} > 0$, thus $\frac{dG_2}{dA} < 0$.
- The function $H(A)$ has a removable singularity at A_S^b and A_U^b, with the limit value at these points $\lim_{A\to A_S,A_U} H(A) = 0$. Thus, $G_2 = 1$ at A_S^b and A_U^b.
- For $A_1^v < A < A_S^b$ the slope of G_2 is negative, and for $A_U^b < A < A_2^v$ the slope of G_2 is positive. As A approaches A_S^b and A_U^b, $1-m(A) \ll 1$ and the second term in the numerator of (48) dominates. Near A_S^b: $\frac{dm(A)}{dA} > 0$ and $1+\gamma-\frac{\gamma}{1-m(A)} < 0$, therefore $\frac{dG_2}{dA} < 0$. Near A_U^b: $\frac{dm(A)}{dA} < 0$, $1+\gamma-\frac{\gamma}{1-m(A)} < 0$, and thus $\frac{dG_2}{dA} > 0$. As A increases from $A = A_U^b$, $\frac{dG_2}{dA}$ remains positive, and $m(A)$ decreases until the curve G_2 reaches an asymptote at A_2^v.

We summarize this information in Figure 1 (b) which shows a qualitative sketch of the curve G_2.

B.1.3. Intersections of G_1 and G_2

Equilibrium points are at intersections between the curves G_1 (45) and G_2 (46). The curve G_1 is in the region $G > 0$ for $A < A_S^b$ and $A_U^b < A < A_{crit}^m$. We will call the region $A < A_S^b$ the lower region and $A_U^b < A$ the upper region.

For $A_1^v < A < A_S^b$ and $A_U^b < A < A_2^v$, curve G_2 is above $G = 1$, thus there can be no intersections with curve G_1 in physically relevant ($x > 0$) regions of phase space.

Intersections between the curves can only occur in the region $A < A_1^v$ and the region $A_2^v < A < 1$.

Intersections in the lower region

The lower branch of G_1 (see figure 45) is a continuous curve connecting the point $(0, G_0)$ and the point $(A_S, b, 0)$, while G_2 is a continuous curve that connects $(0, 1)$ and $(A^t, 0)$. Since $1 > G_0$ to $A_1^t < A_S^b$, thus these curves must intersect at $2n+1$ points, where $n \geq 0$. These correspond to equilibria of the

system and we can order them based on their A value by $E_1, E_2, \ldots E_{2n+1}$. In particular, there is at least one non-trivial equilibrium point between $0 < A < A_1^t$ and $0 < G < max(G_1(A \in (0, A_1^t)))$.

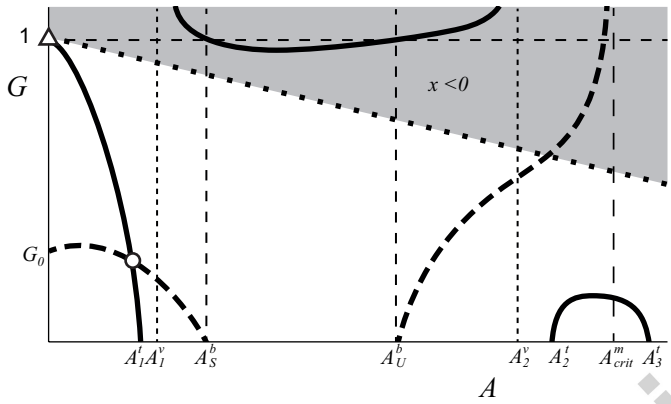

Figure 2: Qualitative sketch of the curves G_1 (dashed black curve) and G_2 (solid black curve). The position of non-trivial equilbrium points projected to (A, G) plane are at the intersections of these curves. Equilibria are marked with a circle for a stable equilibrium point and a triangle for an unstable saddle. The trivial ($x = 0$) equilibrium point at (0,1) is shown. In the shaded grey region ($G > 1 - A/(1+\gamma)$) any solutions are physically unrealistic as $x < 0$. The vertical asymptote of the curve $f(G)I(A) + m(A) = 1$ is labelled A_{crit}^m.

Intersections in the upper region

The upper branch of G_1 is a smooth curve that increases from $G = 0$ at A_U^b until it reaches an asymptote at A defined by $\mu_{1,\max} I(A) + m(A) = 1$. If the curve $1 - \gamma/(1 + \gamma - A)$ intersects $m(A)$ in the upper region, the curve G_2 will cross the A-axis to lie in the $G > 0$ region for $A_2^t < A < A_3^t$, where $A_U^b < A_2^v < A_2^t < A_3^t < 1$. In this case it is possible for the upper branch of the curve G_2 to intersect G_1, thus creating equilibrium points. If these curves do intersect in the upper region, these new upper equilibria, K_j for $j = 1 \ldots 2m$, would appear in pairs at saddle-node bifurcations.

Figure 2 shows the situation when there is an upper branch of G_2, but it doesn't intersect G_1. For there to be equilibrium points in the upper region the upper branch of the curve G_2 must cross the A-axis, and it also must reach high enough G values to intersect with the curve G_1 before G_1 reaches its asymptote at A_{crit}^m.

As was mentioned in the introduction we do not consider these equilibria to represent biologically plausible state of the monoculture. The high stable equilibria only exist in specific circumstances when the acetate growth curve $m(A)$ decreases rapidly for high acetate levels, while the lower stable equilibrium exists for all parameter values. The high stable equilibria, when they exist, have a small basin of attraction, which is characterized by high levels of acetate and

low levels of glucose. So only initial conditions with high initial acetate and low glucose can lead to the monoculture that is positioned at such equilibrium. Below we provide some sufficient conditions under which the curves G_1 and G_2 do not intersect in the upper region and thus there are no equilibria in this region.

1. We expect that the acetate consumer in the binary culture is better adapted to growth on acetate that the monoculture for large value of A. Our fist condition states that the maximal growth rate of monoculture is not greater than a multiple of the growth rate of acetate consumer

$$\mu_{1,\max} I(A_2^v) < \gamma m(A_2^v) \tag{49}$$

where the inequality is evaluated at A_2^v defined implicitly by $m(A_2^v) = \frac{1}{1+\gamma}$. This assumption is summarized in Figure 3. Monotonicity implies that the curve $\mu_{1,\max} I(A)$ is in the shaded region for $A > A_2^v$. The condition (49) comes from the observation that if $I(A_2^v) < \gamma/(\mu_{1,\max}(1+\gamma))$, then $A_{crit}^m < A_2^v$ and the curve G_1 reaches its asymptote before G_2 can enter the region $G > 0$. Therefore there can be no upper equilibria.

2. The second condition which rules out the upper equilibria asks that the function $m(A)$ does not decrease too rapidly for large values of A. Note that if the curve G_2 does not cross the A axis into the $G > 0$ region for upper A values, there can be no upper equilibria. This is equivalent to situation a condition that $m(A) = 1 - \gamma/(1+\gamma-A)$ has no solutions A_2^t and A_3^t, see Figure 3. Finally, observe if

$$m(1) > 1/(1+\gamma) \tag{50}$$

then $1 < A_2^v$ which implies that $m(A) = 1 - \gamma/(1+\gamma-A)$ has only one solution A_1^t. The condition (50) is equivalent to

$$\frac{m\left(\frac{G_{in}Y_{21}}{Y_{11}}\right)}{D} > \frac{Y_{21}}{Y_{21}+Y_{22}}.$$

in terms of the original parameters and variables.

B.2. Stability of equilibrium points

We define a new variable in the monoculture system

$$z(t) = \gamma x(t) + (1+\gamma)G(t) + A(t).$$

It is each to show that

$$\frac{dz}{dt} = (1+\gamma) - z$$

which means that the plane

$$\gamma x + (1+\gamma)G + A = (1+\gamma)$$

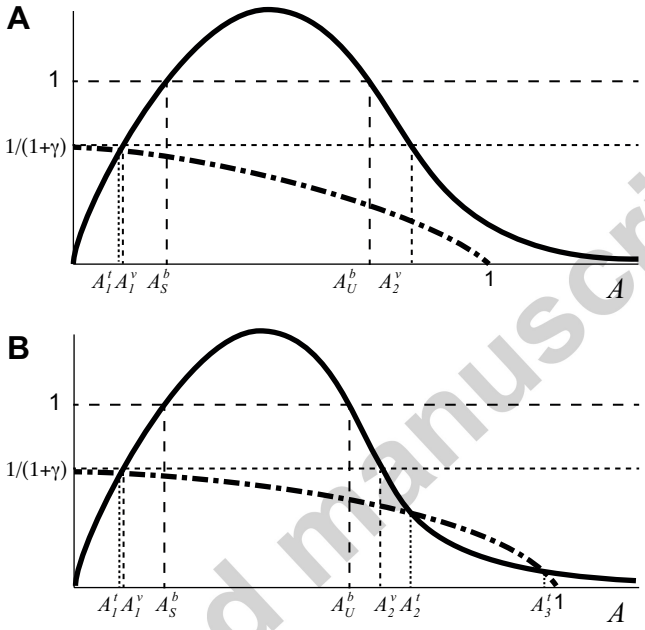

Figure 3: Qualitative sketch of the curves $m(A)$ (solid black curve) and $1-\gamma/(1+\gamma-A)$ (dot-dashed black curve). The case with only one intersection A_1^t is shown in panel (a). In panel (b) the case with three intersections is shown. The A_1^v and A_2^v values which are solutions to $m(A) = 1/(1+\gamma)$ are also shown.

is an attracting (exponentially at a rate of e^{-t}) invariant subspace of the phase space $\mathbb{R}^3_+$.

The long term behavior of the system is determined by the dynamics on this attracting plane, which is given by

$$\frac{dA}{dt} = -A + [f(G)I(A) - \gamma m(A)]\, x(A,G) \tag{51}$$

$$\frac{dG}{dt} = 1 - G - f(G)I(A)x(A,G) \tag{52}$$

$$x(A,G) = \left(1 + \frac{1}{\gamma}\right)(1-G) - \frac{A}{\gamma} \tag{53}$$

This system has the Jacobian

$$J(A,G) = \begin{bmatrix} -1 + \left(f\frac{\partial I}{\partial A} - \gamma\frac{\partial m}{\partial A}\right)x - \frac{1}{\gamma}(fI - \gamma m) & \frac{\partial f}{\partial G}Ix - \left(1+\frac{1}{\gamma}\right)(fI - \gamma m) \\ -f\frac{\partial I}{\partial A}x + \frac{1}{\gamma}fI & -1 - \frac{\partial f}{\partial G}Ix + \left(1+\frac{1}{\gamma}\right)fI \end{bmatrix}.$$

For any 2D system, $tr(J) = \lambda_1 + \lambda_2$ and $det(J) = \lambda_1 \cdot \lambda_2$. The conditions $det(J) > 0$ and $tr(J) < 0$ are necessary and sufficient conditions to show that an equilibrium point is stable. The condition $det(J) < 0$ is necessary and sufficient to show that an equilibrium point is an unstable saddle.

At the trivial equilibrium point, $(A,G) = (0,1)$ where $x = 0$, $I(0) = 1$, and $m(0) = 0$, the Jacobian becomes

$$J(0,1) = \begin{bmatrix} -1 - \left(\frac{1}{\gamma}\right)f(1) & -\left(1+\frac{1}{\gamma}\right)f(1) \\ \left(\frac{1}{\gamma}\right)f(1) & -1 + \left(1+\frac{1}{\gamma}\right)f(1) \end{bmatrix}.$$

The characteristic equation: $\lambda^2 + \lambda(2 - f(1)) + (1 - f(1))$ has roots $\lambda_1 = -1 < 0$, $\lambda_2 = f(1) - 1$. We know that $f(1) \approx \mu_{1,\max} > 1$ from assumption [A6.], so $\lambda_2 > 0$, which means that $(0,1)$ is a saddle, with two negative (stable) eigendirections (one from the reduction to the 2D reduced system and the other from the dynamics of reduced flow) and one unstable eigendirection.

The corresponding eigenvectors are

$$v_1 = \begin{pmatrix} (1+\gamma) \\ -1 \end{pmatrix}, \quad v_2 = \begin{pmatrix} 1 \\ -1 \end{pmatrix}.$$

An important observation to make here is that the stable manifold of the trivial equilibrium point in reduced system is an invariant line $G = 1 - A/(1+\gamma)$ which corresponds to $x = 0$.

Now we analyze the stability of the non-trivial equilibria E_i and K_j. At these equilibria we have $fI + m = 1$, $(fI - \gamma m)x = A$, and $fIx = 1 - G$, with $x(A,G) = (1 + 1/\gamma)(1-G) - A/\gamma$. The Jacobian becomes

$$J(A^m, G^m) = \begin{bmatrix} \left(f\frac{\partial I}{\partial A} - \gamma\frac{\partial m}{\partial A}\right)x - \left(1+\frac{1}{\gamma}\right)fI & \frac{\partial f}{\partial G}Ix + (1+\gamma)\left(1 - \left(1+\frac{1}{\gamma}\right)fI\right) \\ -f\frac{\partial I}{\partial A}x + \frac{1}{\gamma}fI & -1 - \frac{\partial f}{\partial G}Ix + \left(1+\frac{1}{\gamma}\right)fI \end{bmatrix}.$$

The determinant of this Jacobian can (after lengthy rearrangement) be reduced to:

$$\begin{aligned} det(J(A^m, G^m)) =& c_0 \\ =& \frac{\partial f}{\partial G} I \left(\frac{\partial m}{\partial A} \gamma x^2 + fIx \right) - A \left(\frac{\partial m}{\partial A} + f \frac{\partial I}{\partial A} \right). \end{aligned}$$

And the trace of the Jacobian is:

$$\begin{aligned} tr(J(A^m, G^m)) =& - c_1 \\ =& -1 - x \left(\frac{\partial f}{\partial G} I - f \frac{\partial I}{\partial A} + \gamma \frac{\partial m}{\partial A} \right). \end{aligned}$$

To determine the sign of c_0 and thus the stability of any monoculture equilibrium point, we consider the relative slopes of the curves G_1 and G_2 and their intersections in the region $A < A_S^b$. We will show that the stability is determined by the relative slope of the curves G_1 and G_2. Note that at any odd lower equilibrium point $E_i, i = 1, 3, 5, \ldots, 2n+1$ and at any even upper equilibrium point $K_j, j = 2, 4, \ldots 2m$, we have $\frac{\partial G_2}{\partial A} < \frac{\partial G_1}{\partial A}$, whereas at any even lower equilibrium points E_i, $i = 2, 4, 6, \ldots, 2n$, and any odd upper equilibrium points K_j, $j = 1, 3, \ldots 2m-1$, we have $\frac{\partial G_2}{\partial A} > \frac{\partial G_1}{\partial A}$.

Taking the expressions for the slopes from equations (47) and (48), with some rearranging we can show that at non-trivial equilibria

$$A \frac{dG_2}{dA} = -\frac{\partial m}{\partial A} \gamma x^2 - fIx$$

and

$$\frac{\partial f}{\partial G} I \frac{dG_1}{dA} = -\left(\frac{\partial m}{\partial A} + f \frac{\partial I}{\partial A} \right)$$

thus

$$c_0 = \frac{\partial f}{\partial G} I \left(\frac{\partial m}{\partial A} \gamma x^2 + fIx + A \frac{dG_1}{dA} \right) \tag{54}$$

$$= A \frac{\partial f}{\partial G} I \left(\frac{dG_1}{dA} - \frac{dG_2}{dA} \right) \tag{55}$$

- At even lower equilibrium points and odd upper equilibrium points, $\frac{dG_2}{dA} > \frac{dG_1}{dA}$, $c_0 < 0$ and the equilibrium point is an unstable saddle.
- At points where the curves G_1 and G_2 are tangent, $c_0 = 0$ and bifurcations occur.
- At any odd lower equilibrium point and at any even upper equilibrium point $\frac{dG_1}{dA} > \frac{dG_2}{dA}$ and $c_0 > 0$. The equilibrium point in the 2D system is a stable or unstable node, depending on the sign of $tr(J(A^m, G^m))$, which would correspond to a stable node or an unstable saddle in the full system.

For lower even equilibrium points, $tr(J(A^m, G^m)) < 0$ and $c_0 > 0$, so the equilibrium point is a stable node. We can show that these stable equilibria do not undergo Hopf bifurcations (where $Re(\lambda) = 0$) since $tr(J(A^m, G^m)) = \lambda_1 + \lambda_2 \neq 0$.

For upper odd equilibrium points, $c_0 > 0$ but $\frac{\partial m}{\partial A} <$, so the the stability depends on the sign of $tr(J(A^m, G^m))$. If $tr(J(A^m, G^m)) < 0$, then the equilibrium point in the 2D system is a stable node, which corresponds to a stable node in the full system, however, if $tr(J(A^m, G^m)) > 0$, then the equilibrium point in the 2D system is an unstable node, which corresponds to an unstable saddle in the full system.

C. Biomass of monoculture and the binary system

In this section we will prove Theorem 3.

C.1. Comparison of binary culture and monoculture biomass

It can be shown that the biomass $\bar{x}^1 = x_1^1 + x_2^1 = x_1^1 + 0$ for the boundary equilibrium point in the binary system (equations (9)) is always less than the total biomass of the stable co-existence equilibrium point, S: Since $x_1 = 1 - G$ at both equilibria for the binary system, and $G_i^b < G^1$, where G_i^b is the equilibrium glucose concentration for the co-existence equilibria defined below. Thus $\bar{x}^1 < x_{1,i}^b < \bar{x}_i^b$.

In order to compare the maximum biomass in the two systems, we must compare the stable co-existence equilibrium point ($x_1 \neq 0, x_2 \neq 0$) for the binary system with the non-trivial equilibria $E_1, \ldots, E_{2n+1}$ with $x \neq 0$ for the monoculture.

The biomass of the monoculture at equilibrium is given by

$$x^m = \left(1 + \frac{1}{\gamma}\right)(1 - G_i^m) - \frac{A_i^m}{\gamma}. \tag{56}$$

The total biomass of the binary system at its stable equilibrium point $\bar{x}_S^b = x_{1,S}^b + x_{2,S}^b$:

$$\bar{x}_S^b = \left(1 + \frac{1}{\gamma}\right)(1 - G_S^b) - \frac{A_S^b}{\gamma}. \tag{57}$$

As shown in B, $A_i^m < A_t < A_S^b$ for all monoculture equilibria in the region (on the lower $A < A_b^S$ branch).

The slope of curve implicitly defined by $f(G)I(A) = 1$, on which G_S^b lies, is given by equation (30). The curve G_1, on which G_i^m lies, has slope given by equation (47). Both curves intersect the G-axis at $G = G_0$. The slope for the binary culture curve (equation (30)) is always larger than the slope of the monoculture curve (equation (47)) in the region $A < A_{\max}$, as $\frac{\partial m}{\partial A} > 0$. Thus, in the region $A < A_t$, the monoculture curve G_1 lies below the binary culture curve implicitly defined by $f(G)I(A) = 1$ and $G_i^m < G_S^b$.

As $A_i^m < A_S^b$ and $G_i^m < G_S^b$, from equations (56) and (57) we know that $x^m > \bar{x}_S^b$. In other words, given these assumptions, the monoculture will always have greater biomass than the binary culture (division of labour system).

D. Experimental values for *E. coli* growth

Table 4 details the experimental conditions and strains used for the parameters listed in Table 1. When the reported constants were obtained by fitting data to a specific model, we report the equivalent observable values. The maximum growth rates are the maximum values of the growth function on that substrate, assuming zero inhibitory products. The half-saturation values are the substrate concentration at which the growth has reached half its maximum value. The acetate product inhibition constant we define as the acetate concentration at which the growth rate has decreased to half its maximum value, in excess glucose ($G \gg K_G$). The acetate substrate inhibition constant we define as the acetate concentration at which the growth rate has decreased to half its maximum value.

Source	Strain	Experimental conditions	Parameter	Val
Bernstein *et al.* (2012) [3]	*E. coli* MG1655 WT mutant 307 mutant 403	Aerobic batch growth, 37°C, M9 minimal media, acetate consumption deletion glucose consumption deletion	Biomass yield (CDW[g]/g of glucose) Maximum growth rate on 4g/L glucose (h^{-1}) Maximum growth rate on 1.5g/L acetate (h^{-1})	0. 0.43- 0.11-
Chen *et al.* (1997) [7]	*E. coli* K-12 MG1655	Aerobic batch growth, complex medium, 37°C	Maximum growth rate on glucose (h^{-1}) Biomass yield (CDW[g]/g of glucose)	0. 0.
Chen *et al.* (1997) [7]	*E. coli* K-12 MG1655	Anaerobic batch growth, complex medium, 37°C	Maximum growth rate on glucose (h^{-1}) Biomass yield (CDW[g]/g of glucose)	0. 0.
Dykhuizen (1978) [11]	*E. coli* K-12 W3110	Aerobic batch growth, Davis salts, 37°C	Maximum growth rate on glucose (h^{-1})	0.
Dykhuizen (1978) [11]	*E. coli* K-12 W3110	Chemostat growth, Davis salts, 37°C	Glucose half-saturation constant (mg/L)	7.
Edwards *et al.* (2001) [12]	*E. coli* K-12 MG1655	Aerobic batch growth, M9 minimal media 27.5-37°C, 0.05-4 g/L acetate	Maximum growth rate on acetate (h^{-1}) Biomass yield (CDW[g]/g of acetate)	0. 0.
Farmer and Liao (1997) [17]	*E coli* K-12 VJS632	Aerobic batch growth, 37°C, M9 minimal media, 0.5% glucose	Maximum growth rate on glucose (h^{-1}) Biomass yield (CDW[g]/g of glucose) Acetate yield (g of acetate/g of glucose)	0. 0. 0.
Review paper [18]	*E. coli* various	various	Glucose half-saturation constant (mg/L)	0.04-
Fuhrer *et al.* (2005) [20]	*E. coli* K-12 MG1655	Aerobic batch growth, 30°C, M9 minimal media, 3g/L glucose	Maximum growth rate on glucose (h^{-1}) Biomass yield (CDW[g]/g of glucose)	0. 0.
Guardia and Calvo (2001) [23]	*E. coli* ATCC 8789	Aerobic batch and chemostat growth, 37°C, complex medium including 5g/L yeast extract, varying 1-19g/L glucose, parameter fits to model	Maximum growth rate on glucose (h^{-1}) Glucose half-saturation constant (mg/L) Acetate product inhibition constant (g/L) Maximum growth rate on acetate (h^{-1}) Acetate half-saturation constant (g/L) Acetate substrate inhibition constant (g/L) Acetate yield (g acetate produced/CDW[g])	1. 10 4 0. 0. 3. 0.
Kleman and Strohl (1994) [32]	*E. coli* K-12 W3110	Aerobic fed-batch with target 0.5g/L glucose, mineral medium, 35°C	Maximum growth rate on glucose (h^{-1}) Glucose half-saturation constant (mg/L) Biomass yield (CDW[g]/g of glucose) Acetate yield (g of acetate/g of glucose) Acetate yield (g acetate produced/CDW[g])	0. 4 0. 0. 0.3-

Source	Strain	Experimental conditions	Parameter	Val
Natarajan and Srienc (2000) [40]	*E. coli* BL21	Chemostat, 30°C, dilution rate 0.12-0.40 h^{-1} inflow: M9 minimal media, 0.25g/L glucose	Maximum growth rate on glucose (h^{-1}) Glucose half-saturation constant (mg/L)	0.7 0.6
Oh *et al.* (2002) [42]	*E. coli* MC4100	Aerobic batch growth, M9 minimal media	Maximum growth rate on 0.25% acetate (h^{-1})	0.3
Paalme *et al.* (1997) [43]	*E. coli* K-12 W3350	A-stat, 37°C, mineral medium, 10g/L glucose	Maximum growth rate on glucose (h^{-1}) Biomass yield (CDW[g]/g of glucose)	0.5 0.5
Paalme *et al.* (1997) [43]	*E. coli* K-12 W3350	A-stat, 37°C, mineral medium, 5g/L acetate	Maximum growth rate on acetate (h^{-1}) Biomass yield (CDW[g]/g of acetate) max/min	0.2 0.30/
Senn *et al.* (1994) [59]	*E. coli* ML30	Chemostat growth, mineral medium, 37°C	Maximum growth rate on glucose (h^{-1}) Glucose half-saturation constant (mg/L)	0.9 0.00
Literature review [59]	*E. coli* various	various	Maximum growth rate on glucose (h^{-1}) Glucose half-saturation constant (mg/L)	0.55- 0.005
Varma and Palsson (1994) [65]	*E. coli* K-12 W3110	Aerobic batch growth, 38°C, M9 minimal media, 2 g/L glucose	Maximum growth rate on glucose (h^{-1}) Biomass yield (CDW[g]/g of glucose)	0.6 0.3
Varma and Palsson (1994) [65]	*E. coli* K-12 W3110	Anaerobic batch growth, 38°C, M9 minimal media, 2 g/L glucose	Maximum growth rate on glucose (h^{-1}) Biomass yield (CDW[g]/g of glucose)	0.4 0.1
Xu, Jahic, and Enfors (1999) [69]	*E. coli* K-12 W3110	Aerobic batch growth, 35°C, mineral medium, 4-14 g/L glucose	Maximum growth rate on glucose (h^{-1}) Biomass yield (CDW[g]/g of glucose) Maximum growth rate on acetate (h^{-1})	0.5 0.5 0.0
Xu, Jahic, and Enfors (1999) [69]	*E. coli* K-12 W3110	Aerobic batch growth, 35°C, mineral medium, 5 g/L glucose, 0-8 g/L acetate	Acetate product inhibition constant (g/L) Biomass yield (CDW[g]/g of acetate)	9 0.4
Xu, Jahic, and Enfors (1999) [69]	*E. coli* K-12 W3110	Aerobic fed-batch (exponential feeding rate) with target $\mu = 0.3h^{-1}$, mineral medium, 35°C	Maximum growth rate on glucose (h^{-1}) Glucose half-saturation constant (mg/L) Acetate product inhibition constant (g/L) Aerobic biomass yield (CDW[g]/g of glucose) Anaerobic biomass yield (CDW[g]/g of glucose) Maximum growth rate on acetate (h^{-1}) Acetate half-saturation constant (g/L) Biomass yield (CDW[g]/g of acetate)	0.5 50 4, 0.49, 0.1 0.06, 0.0 0.4

Table 4: Typical parameter values for *E. Coli* growth. [a](before - after) adaptation to a single carbon source. Note: When parameters were from the fit to a specific inhibition model, the parameters reported in are the 'effective' parameters, i.e., the reported 'inhibition constants' are the concentration at which growth rate has decreased to half its maximum. Similarly, the 'half-saturation constants' are the concentrations at which growth has increased to half its maximum, and the 'maximum growth rates' are the maximum possible growth rates.

References

References

[1] Abrams, P., 1987. The Functional Responses of Adaptive Consumers of Two Resources. Theoretical Population Biology 32, 262–288.

[2] Aota, Y., Nakajima, H., 2001. Mutualistic relationships between phytoplankton and bacteria caused by carbon excretion from phytoplankton. Ecological Research 16, 289–299.

[3] Bernstein, H., Paulson, S., Carlson, R., 2012. Synthetic *Escherichia coli* consortia engineered for syntrophy demonstrate enhanced biomass productivity. Journal of Biotechnology 157, 159–166.

[4] Brown, T.D.K., Jones-Mortimer, M.C., Kornberg, H.L., 1977. The Enzymic Interconversion of Acetate and Acetyl-coenzyme A in *Escherichia coli*. Journal of General Microbiology 102, 327–336.

[5] Burchard, A., 1994. Substrate degradation by a mutualistic association of two species in the chemostat. Journal of Mathematical Biology 32, 465–489.

[6] Carlson, R., Srienc, 24. Fundamental *Escherichia coli* biochemical pathways for biomass and energy production: Creation of overall flux states. Biotechnology and Bioengineering 85, 149–162.

[7] Chen, R., Yap, W., Postma, P., Bailey, J., 1997. Comparative studies of *Escherichia coli* strains using different glucose uptake systems: Metabolism and energetics. Biotechnology and Bioengineering 56, 583–590.

[8] Costa, E., Perez, J., Kreft, J., 2006. Why is metabolic labour divided in nitrification? TRENDS in Microbiology 14, 213–219.

[9] DeLong, J., 2008. The maximum power principle predicts the outcomes of two-species competition experiments. Oikos 117, 1329–1336.

[10] Doebeli, M., 2002. A model for the evolutionary dynamics of cross-feeding polymorphisms in microorganisms. Population Ecology 44, 59–70.

[11] Dykhuizen, D., 1978. Selection for Tryptophan Auxotrophs of Escherichia coli in Glucose-Limited Chemostats as a Test of the Energy Conservation Hypothesis of Evolution. Evolution 32, 125–150.

[12] Edwards, J.S., Ibarra, R.U., Palsson, B.O., 2001. *In silico* predictions of *Escherichia coli* metabolic capabilities are consistent with experimental data. Nature Biotechnology 19, 125–130.

[13] Egli, T., Lendenmann, U., Snozzi, M., 1993. Kinetics of microbial growth with mixtures of carbon sources. Antonie van Leeuwenhoek 63, 289–298.

[14] Eiteman, M., Lee, S., Altman, E., 2008. A co-fermentation strategy to consume sugar mixtures effectively. Journal of Biological Engineering 2, 3.

[15] Elkhader, A., 1991. Global stability in a synthrophic chain model. Mathematical Biosciences 104, 203–245.

[16] Estrela, S., Gudejl, I., 2010. Evolution of cooperative cross-feeding could be less challenging than originally thought. PLoS One 5, e14121.

[17] Farmer, W.R., Liao, J.C., 1997. Reduction of aerobic acetate production by *Escherichia coli*. Applied and Environmental Microbiology 63, 3205–3210.

[18] Ferenci, T., 1996. Adaptation to life at micromolar nutrient levels: the regulation of *Escherichia coli* glucose transport by endoinduction and cAMP. FEMS Microbiology Reviews 18, 301–317.

[19] Fierer, N., Jackson, R., 2006. The diversity and biogeography of soil bacterial communities. PNAS 103, 626–631.

[20] Fuhrer, T., Fischer, E., Sauer, U., 2005. Experimental identification and quantification of glucose metabolism in seven bacterial species. Journal of Bacteriology 187, 1581–1590.

[21] Gardner, S., Hillis, S., Heilmann, K., Segre, J., Grice, E., 2013. The neuropathic diabetic foot ulcer microbiome is associated with clinical factors. Diabetes 62, 923–930.

[22] Gill, S., Pop, M., DeBoy, R., Eckburg, P., Turnbaugh, P., Samuel, B., Gorden, J., Relman, D., Fraser-Liggett, C., Nelson, K., 2006. Metagenomic analysis of the human distal gut microbiome. Science 312, 1355–1359.

[23] Guardia, M.J., Calvo, E.G., 2001. Modeling of *Escherichia coli* growth and acetate formation under different operational conditions. Enzyme and Microbial Technology 29, 449–455.

[24] Han, K., Levenspiel, O., 1988. Extended Monod kinetics for substrate, product, and cell inhibition. Biotechnology and bioengineering 32, 430–447.

[25] Han, K., Lim, H., Hong, J., 1992. Acetic acid formation in *Escherichia coli* fermentation. Biotechnology and Bioengineering 39, 663–671.

[26] Hardin, G., 1960. The competitive exclusion principle. Science 131, 1292–1297.

[27] Helling, R.B., Vargas, C.N., Adams, J., 1987. Evolution of *Escherichia coli* during growth in a constant environment. Genetics 116, 349–358.

[28] Ibarra, R.U., Edwards, J., Palsson, B., 2002. *Escherichia coli* K-12 undergoes adaptive evolution to achieve *in silico* predicted optimal growth. Nature 420, 186–189.

[29] James, G., Swogger, E., Wolcott, R., deLancey Pulcini, E., Secor, P., Sestrich, J., Costerton, J., Stewart, P., 2008. Biofilms in chronic wounds. Wound Repair and Regeneration 16, 37–44.

[30] Johnson, D., Goldschmidt, F., Lilja, E., Ackermann, M., 2012. Metabolic specialization and the assembly of microbial communities. The ISME Journal doi: 10.1038/ismej.2012.46, 1–7.

[31] Katsuyama, C., Nakaoka, S., Takeuchi, Y., Tago, K., Hayatsu, M., Kato, K., 2009. Complementary cooperation between two syntrophic bacteria in pesticide degradation. Journal of Theoretical Biology 256, 644–654.

[32] Kleman, G.L., Strohl, W.R., 1994. Acetate metabolism by *Escherichia coli* in high-cell-density fermentation. Applied and Environmental Microbiology 60, 3952–3958.

[33] Kreikenbohm, R., Bohl, E., 1986. A mathematical model of syntrophic cocultures in the chemostat. FEMS Microbiology Ecology 38, 131–140.

[34] Kumari, S., Tichel, R., Eisenbach, M., Wolfe, A.J. 1995. Cloning, characterization, and functional expression of *acs*, the gene which encodes acetyl coenzyme A synthetase in *Escherichia coli*.. Journal of Bacteriology 177, 2878–2886.

[35] Lendenmann, U., Egli, T., 1922. Kinetic Models for the Growth of Escherichia coli with Mixtures of Sugars under Carbon-Limited Conditions. Biotechnology and bioengineering 59, 99–107.

[36] Lotka, A., 1922. Contribution to the energetics of evolution. PNAS 8, 147–151.

[37] MacArthur, R., Levins, R., 1964. Competition, habitat selection, and character displacement in a patchy environment. PNAS 51, 1207–1210.

[38] de Mazancourt, C., Schwartz, M.W., 2010. A resource ratio theory of cooperation. Ecology Letters 13, 349–359.

[39] Miller, T., Burns, J., Munguia, P., Walters, E., Kneitel, J., Richards, P., Mouquet, N., Buckley, H., 2005. A critical review of twenty years' use of the resource-ratio theory. The American Naturalist 165, 439–448.

[40] Natarajan, A., Srienc, F., 2000. Glucose uptake rates of single *Escherichia coli* cells grown in glucose-limited chemostat cultures. Journal of Microbiological Methods 42, 87–96.

[41] Nicolaou, S.A., Gaida, S.M.,Papoutsakis, E.T., 2010. A comparative view of metabolite and substrate stress and tolerance in microbial bioprocessing: from biofuels and chemicals, to biocatalysis and bioremediation. Metabolic Engineering 12, 307–331.

[42] Oh, M., Rohlin, L., Kao, K., Liao, J., 2002. Global expression profiling of acetate-grown *Escherichia coli*. The Journal of Biological Chemistry 277, 13175–13183.

[43] Paalme, T., Elken, R., Kahru, A., Vanatalu, K., Vilu, R., 1997. The growth rate control in *Escherichia coli* at near to maximum growth rates: the A-stat approach. Antonie van Leeuwenhoek 71, 217–230.

[44] Peralta-Yahya, P., Zhang, F., del Cardayre, S., Keasling, J., 2012. Microbial engineering for the production of advanced biofuels. Nature 488, 320–328.

[45] Pfeiffer, T., Bonhoeffer, S., 2004. Evolution of cross-feeding in microbial populations. The American Naturalist 163, E126–E135.

[46] Powell, G., 1985. Stable coexistence of syntrophic associations in continuous culture. Journal of Chemical Technology and Biotechnology 35B, 46–50.

[47] Powell, G., 1986. Stable coexistence of synthrophic chains in continuous culture. Theoretical Population Biology 30, 17–25.

[48] Reilly, P., 1974. Stability of commensalistic systems. Biotechnology and Bioengineering 16, 1373–1392.

[49] Rescigno, A., Richardson, I., 1965. On the competitive exclusion principle. Bulletin of Mathematical Biology 27, 85–89.

[50] Rosenzweig, F., Sharp, R., Treves, D., Adams, J., 1994. Microbial evolution in a simple unstructured environment: Genetic differentiation in *Escherichia coli*. Genetics 137, 903–917.

[51] Rozen, D., Lenski, R., 2000. Long-term experimental evolution in *Escherichia coli*. VIII. dynamics of a balanced polymorphism. The American Naturalist 155, 24–35.

[52] Sari, T., El Hajji, M., Harmand, J., 2012. The mathematical analysis of a syntrophic relationship between two microbial species in a chemostat. Mathematical Biosciences and Engineering 9, 627–645.

[53] Schink, B., 1997. Energetics of syntrophic cooperation in methanogenic degradation. Microbiology and molecular biology reviews 61, 262–280.

[54] Schink, B., 2002. Synergistic interactions in the microbial world. Antonie van Leeuwenhoek 81, 257–261.

[55] Schuster, S., Pfeiffer, T., Fell, D., 2008. Is maximization of molar yield in metabolic networks favoured by evolution? Journal of Theoretical Biology 252, 497–504.

[56] Sciubba, E., 2011. What did Lotka really say? A critical reassessment of the "maximum power principle". Ecological Modelling 222, 1347–1353.

[57] Seitz, H., Schink, B., Pfennig, N., Conrad, R., 1990a. Energetics of syntrophic ethanol oxidation in defined chemostat cocultures: 1. Energy requirement for H_2 production and H_2 oxidation. Archives of Microbiology 155, 82–88.

[58] Seitz, H., Schink, B., Pfennig, N., Conrad, R., 1990b. Energetics of syntrophic ethanol oxidation in defined chemostat cocultures: 2. Energy sharing in biomass production. Archives of Microbiology 155, 89–93.

[59] Senn, H., Lendenmann, U., Snozzi, M., Hamer, G., Egli, T., 1994. The growth of *Escherichia coli* in glucose-limited chemostat cultures: a reexamination of the kinetics. Biochimica et Biophysica Acta 1201, 424–436.

[60] Shong, J., Diaz, M., Collins, C., 2012. Towards synthetic microbial consortia for bioprocessing. Current Opinion in Biotechnology 23, 1–5.

[61] Smith, H., Waltman, P., 1995. The Theory of the Chemostat. Cambridge University Press.

[62] Tilman, D., 1982. Resource Competition and Community Structure. Princeton University Press, Princeton, N.J., U.S.A.

[63] Tilman, D., 1988. Dynamics and Structure of Plant Communities. Princeton University Press, Princeton, N.J., U.S.A.

[64] Treves, D., Manning, S., Adams, J., 1998. Repeated evolution of an acetate-crossfeeding polymorphism in long-term populations of *Escherichia coli*. Molecular Biology and Evolution 15, 789–797.

[65] Varma, A., Palsson, B.O., 1994. Stoichiometric flux balance models quantitatively predict growth and metabolic by-product secretion in wild-type *Escherichia coli* W3110. Applied and Environmental Microbiology 60, 3724–3731.

[66] Venter, J., Remington, K., Heidelberg, J., Halpern, A., Rusch, D., Eisen, J., Wu, D., Paulsen, I., Nelson, K., Nelson, W., Fouts, D., Levy, S., Knap, A., Lomas, M., Nealson, K., White, O., Peterson, J., Hoffman, J., Parsons, R., Baden-Tillson, H., Pfannkock, C., Rogers, Y., Smith, H.O., 2004. Environmental genome shotgun sequencing of the sargasso sea. Science 304, 66–74.

[67] Wintermute, E., Silver, P., 2010. Emergent cooperation in microbial metabolism. Molecular Systems Biology 6, 407.

[68] Wolfe, A., 2005. The acetate switch. Microbiology and molecular biology reviews 69, 12.

[69] Xu, B., Jahic, M., Enfors, S., 1999. Modeling of overflow metabolism in batch and fed-batch cultures of *Escherichia coli*. Biotechnology Progress 15, 81–90.

[70] Zuroff, T., Curtis, W., 2012. Developing symbiotic consortia for lignocellulosic biofuel production. Applied Microbiology and Biotechnology 93, 1423–1435.